

Electron-Driven Chemistry: How Resonances Drive e⁻-Molecule Collisions

T. N. Rescigno

Lawrence Berkeley National Lab

Collaborators: C. W. McCurdy (LBL)

A. E. Orel (UC Davis)

H-D. Meyer (University of Heidelberg)

Zhiyong Zhang (LBL)

Wim Vanroose (LBL)

Dan Haxton (UC Berkeley)



Electronic Collisions Drive a Multitude of Common Physical Devices and Chemical Changes

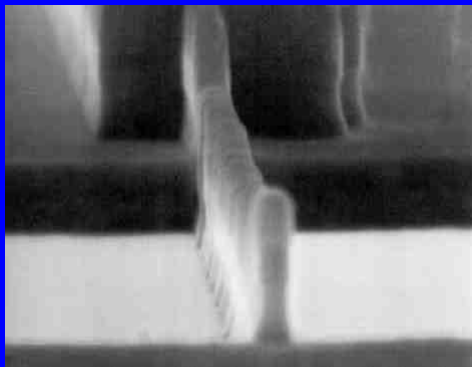


**High Intensity Plasma
Arc Lamp (OSRAM-
Sylvania)**

Electronic collisions are uniquely effective in transferring energy to and from the electronic degrees of freedom of the target atom or molecule. That is the fundamental reason that new developments in modern fluorescent lighting and plasma displays are distinguished by their energy efficiency.



**Plasma Flat Panel
Display (Fujitsu)**



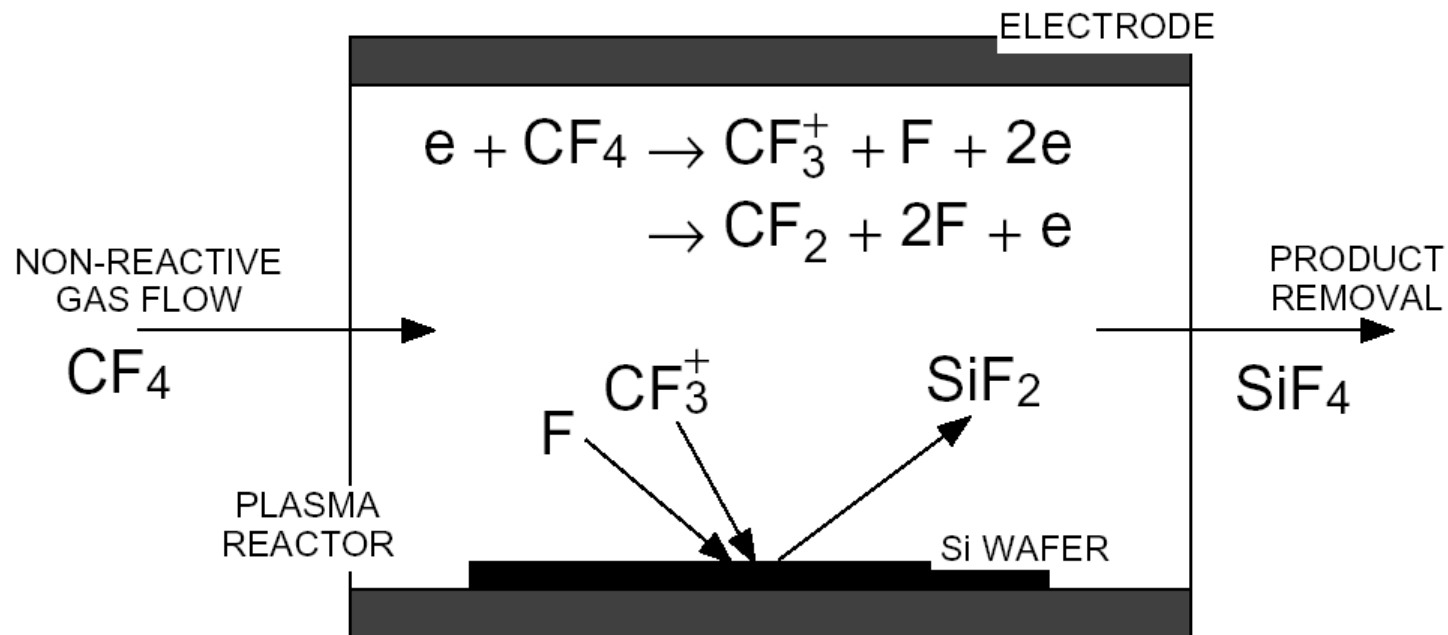
**Plasma-etched Gate
0.12 microns wide,
(Bell Labs --Lucent
Technologies)**

The molecules used to etch semiconductor materials do not react with silicon surfaces unless they are subjected to electronic collisions in the low-temperature, high-density plasmas used in plasma etching and plasma enhanced chemical vapor deposition.

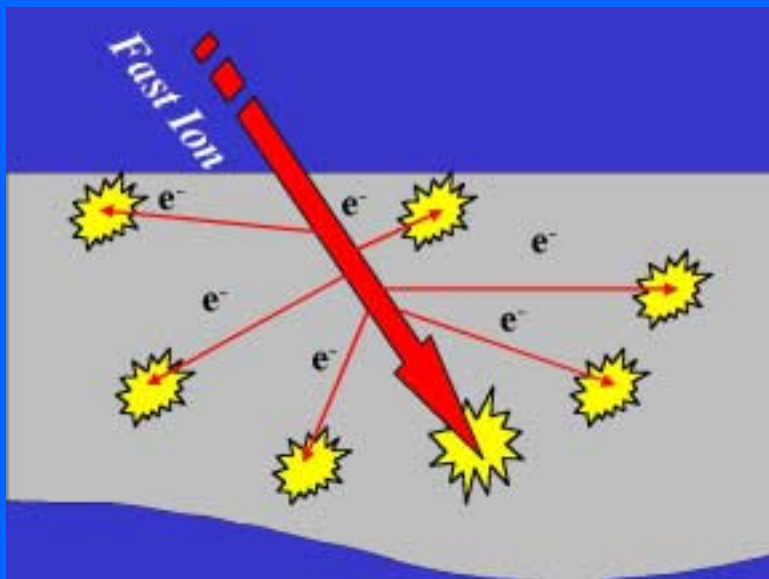
Example: Plasma vapor deposition and Plasma Etching

No chemistry without electrons from plasma discharge

- Polycrystalline silicon and silicon dioxide etching: Cl_2 , Br_2 , HBr , O_2 , N_2 , BCl_3 , HCl , CF_4 , CHF_3 , C_2F_6 , C_3F_8 , C_4F_8 , NF_3
- Silicon deposition SiH_4 , N_2O , Ar , $\text{TEOS}[\text{C}_2\text{H}_4\text{O}]_4$
- Metal deposition: Cu , Al , Ti , Ba , W , Sr



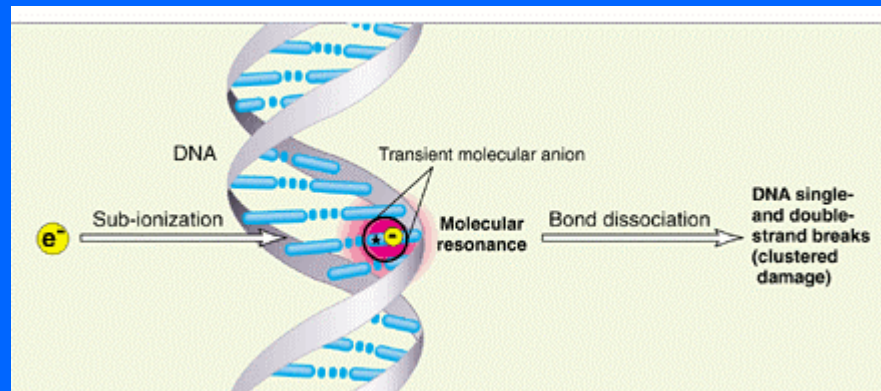
Electron-Driven Chemistry Associated with Ionizing Radiation



Cascades of secondary electrons
from ionizing radiation

Low energy electrons with energies significantly below the ionization energies of DNA molecules can initiate single and double strand-breaks by attaching to components of DNA molecules or the water around them and driving bond dissociation.

Secondary electron cascades in mixed radioactive/ chemical waste drive much of the chemistry that determines how those materials age, change, and interact with the natural environment.



Most energy deposited in cells by ionizing radiation is channeled into secondary electrons between 1eV and 20eV (Research group of L. Sanche)

Secondary electrons play a pivotal role in radiation damage

- Dissociative attachment and resonant processes occur primarily for electron energies below 20 eV
- The energy distribution of secondary electrons emphasizes those processes

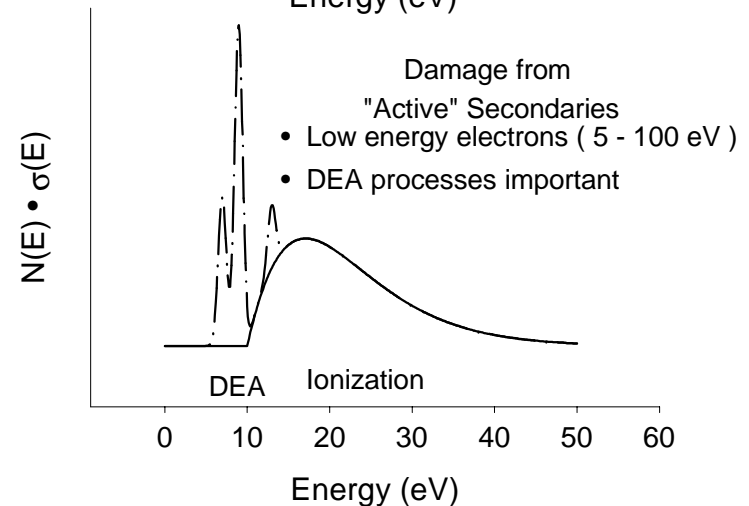
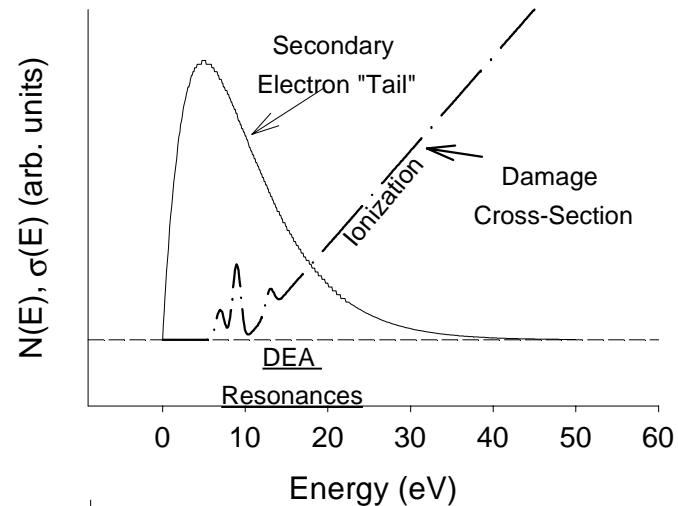


Figure from Thom Orlando, Ga Tech

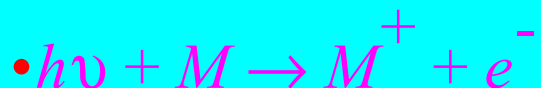
Electron Impact Processes

- $e^{-} + M \rightarrow e^{-} + M^{*}$ **Electronic excitation** (Any symmetry *and* singlet to singlet *and* singlet to triplet)
- $e^{-} + M \rightarrow e^{-} + A + B$ **Electron impact dissociation**
- $e^{-} + M \rightarrow A^{-} + B$ **Dissociative attachment**
- $e^{-} + M \rightarrow e^{-} + e^{-} + M^{+}$ **Electron impact ionization**

Contrast photoexcitation and photoionization



Optical Selection Rules



Nuclear Dynamics - Resonant and Non-Resonant Collisions

- **Electron-driven chemistry hinges on the mechanisms by which electronic energy is transferred into nuclear motion to produce reactive species by excitation and/or fragmentation**

Non-resonant collisions - electronic excitation

- **$m_e/M \sim 10^{-3} \Rightarrow$ disparate collisional time scales \Rightarrow impulsive electronic excitation followed by nuclear fragmentation - electron dynamics and nuclear dynamics decouple**

Resonant collisions

- **electron collision times commensurate with a molecular vibrational period**
- **electron collisions drive vibrational excitation, dissociative attachment, dissociative recombination**
- **formal resonance theory - multidimensional nuclear motion in polyatomics can lead to new effects**

***Ab Initio* Electron-Molecule Scattering**

The problem: From first principles, solve the scattering problem including the nuclear dynamics, predict the cross sections and show how they display the underlying dynamics of the collision.

- **Breaking up the problem into two parts:**
 - A. Electron scattering for fixed nuclei: Calculate the position and lifetime of the shape or Feshbach resonances
 - B. Nuclear dynamics during the resonant collision: Calculate the quantum molecular dynamics leading to vibrational excitation or dissociative attachment

Computational Electron-Molecule Scattering – the fixed-nuclei electronic problem

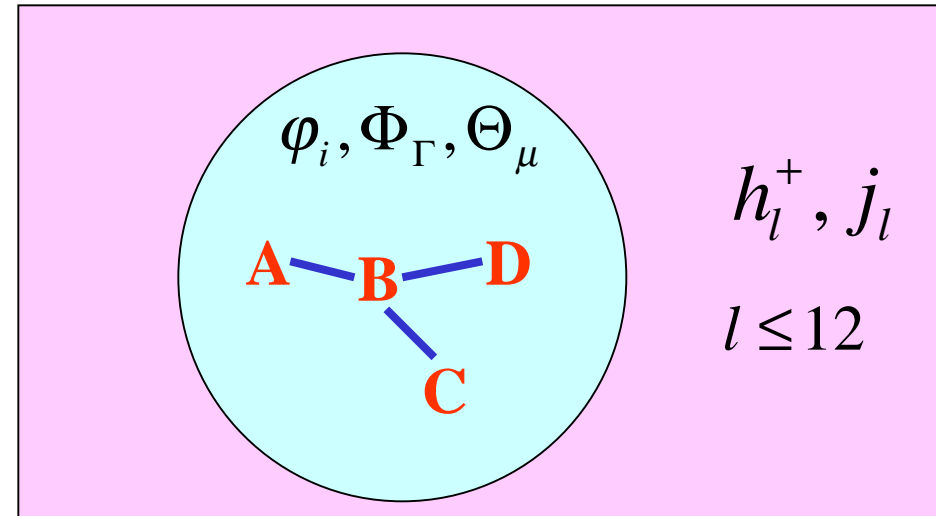
- At the low collision energies of interest to EDC, incident electron and target electrons are indistinguishable – electronic *structure* and electron *dynamics* are inseparable.
- The key to a successful approach is the interface between electronic structure and electron dynamics.
- Virtually all successful modern approaches are *variational*.
- Our approach is based on the complex Kohn variational method – a Hamiltonian – based, anomaly-free approach that allows us to fully exploit the rich infrastructure of bound-state quantum chemistry

Complex Kohn Variational Method

Variational Functional for the
T-Matrix (scattering amplitude)

$$[T^{\Gamma\Gamma_0}] = T^{\Gamma\Gamma_0} - 2 \int \Psi_{\Gamma} (H - E) \Psi_{\Gamma_0}$$

$$\delta[T] = 0$$



Trial wave function for the N+1 electron system

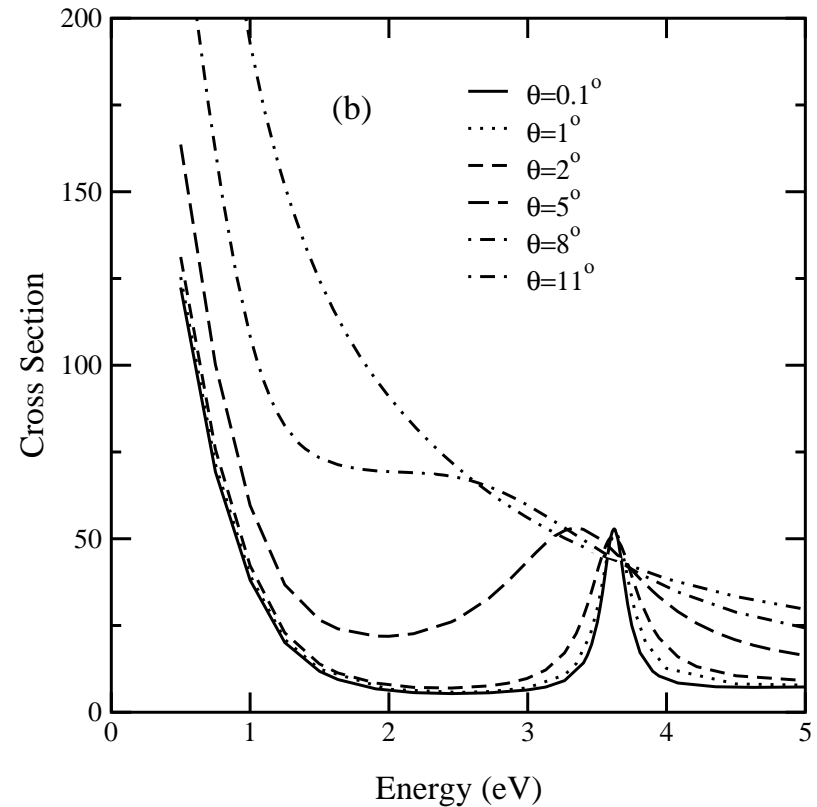
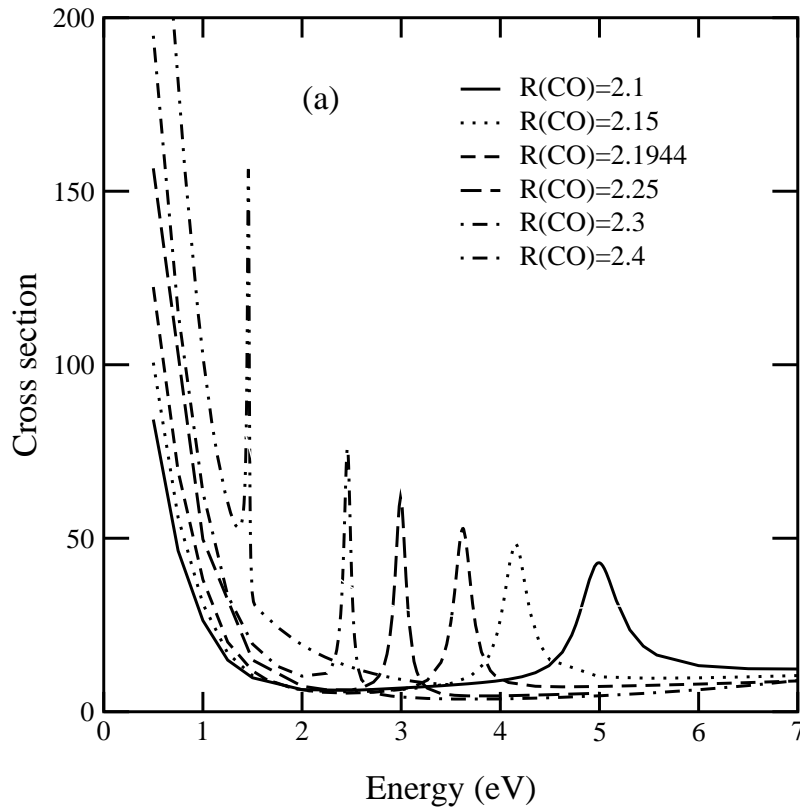
$$\Psi_{\Gamma_0} = \sum_{\Gamma} A \{ \Phi_{\Gamma}(\mathbf{r}_1 \cdots \mathbf{r}_N) F_{\Gamma\Gamma_0}(\mathbf{r}_{N+1}) \} + \sum_{\mu} d_{\mu}^{\Gamma_0} \Theta_{\mu}(\mathbf{r}_1 \cdots \mathbf{r}_{N+1})$$

↑
exchange
↑
target
↑
continuum
↑
Correlation and Polarization

Continuum functions are further expanded in combined basis of Gaussians
and continuum functions

$$F_{\Gamma\Gamma_0}(\mathbf{r}) = \sum_i c_i^{\Gamma\Gamma_0} \varphi_i(\mathbf{r}) + [j_l(k_{\Gamma}r) \delta_{ll_0} \delta_{mm_0} + T_{ll_0mm_0}^{\Gamma\Gamma_0} h_l^+(k_{\Gamma}r)] Y_{l,m}(\hat{\mathbf{r}}) / r$$

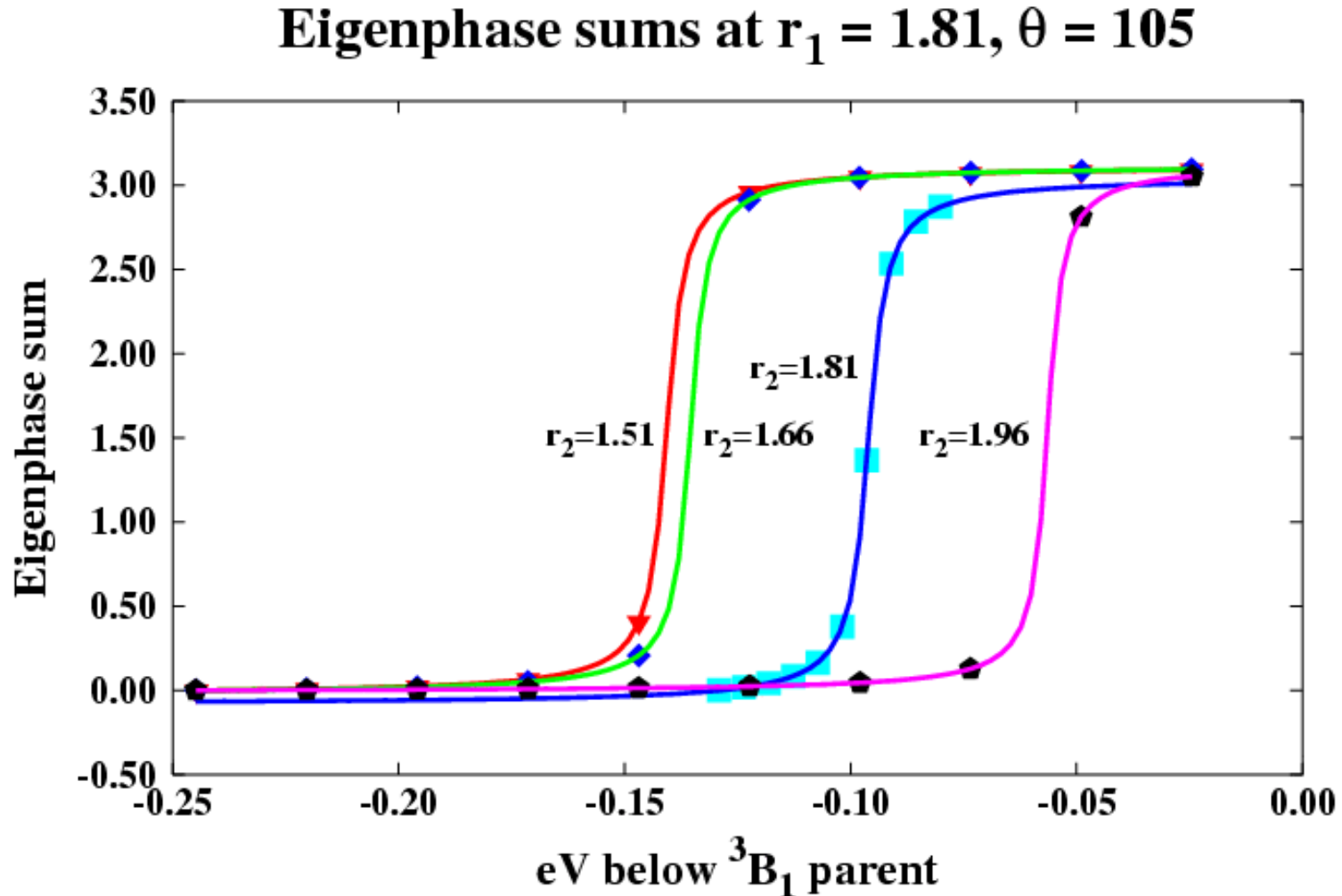
Fixed Nuclei Electron-Scattering Cross sections in 2A_1 symmetry for varying geometries



Resonance feature gives a **position and width**: A complex energy for the resonance $E_{res}(R) = E_r - i\Gamma/2$ which can be understood in the simplest interpretation via

$$|\Psi(r, t)|^2 = |\psi(r)e^{-iE_{res}t}|^2 = |\psi(r)|^2 e^{-\Gamma t}$$

E_R and Γ are determined from the eigenphase sums in the Complex Kohn calculation near the resonance



E.g. at equilibrium geometry $\Gamma = 0.005819\text{eV}$

The Nuclear Dynamics: Formulation of the problem

- Partition the total wave function into resonant and non-resonant components
- For a **single, isolated resonance**, use Born-Oppenheimer approximation for both resonance and nonresonant background
- The T-matrix (scattering amplitude) for vibrational excitation (or dissociative attachment) is given by the nuclear wave equation

$$[E - E_{res}(R) - K_R]\xi(\mathbf{R}) = \langle \psi_{res} | H_{el} | P \phi_{v_i}^+ \rangle + \langle \psi_{res} | H_{el} P G^+ P H_{el} | \psi_{res} \rangle \xi(\mathbf{R})$$

A series of approximations converts this essentially exact equation into the “Boomerang” or “local complex potential” approximation

Local Complex Potential or “Boomerang” Approximation

Time-independent formulation:

$$\{E - H_{anion}\} \xi(\mathbf{R}) = \Phi_{initial}(\mathbf{R})$$

$$\Phi_{initial}(\mathbf{R}) = \left(\frac{\Gamma(\mathbf{R})}{2\pi} \right)^{1/2} \chi_i(\mathbf{R})$$

Hamiltonian for nuclear motion of anion with local complex potential

$$H_{anion} = K_R + [E_{res}(\mathbf{R}) - i\Gamma(\mathbf{R})/2]$$

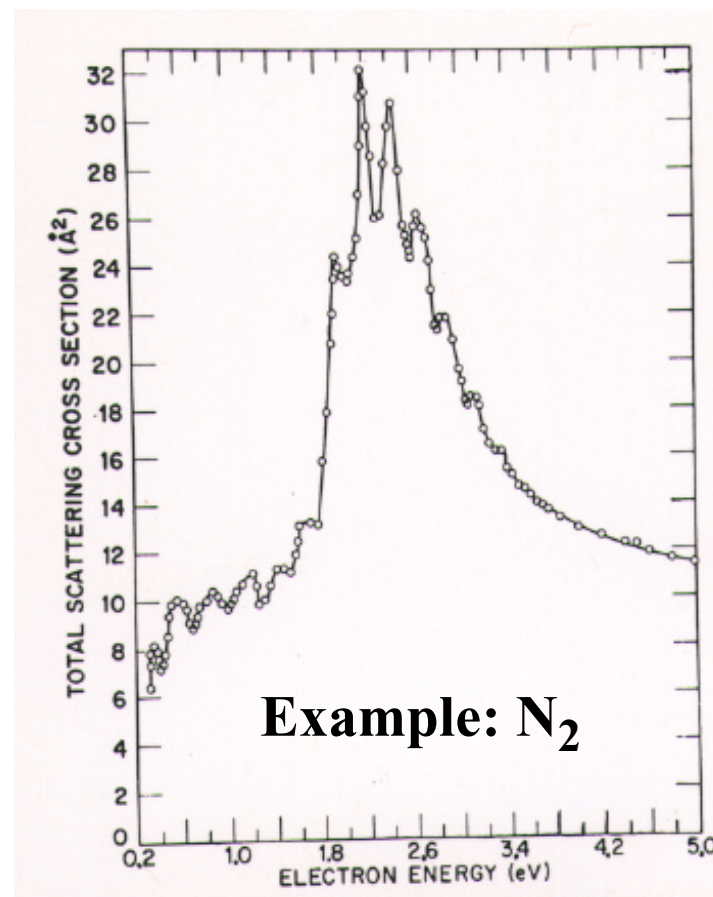
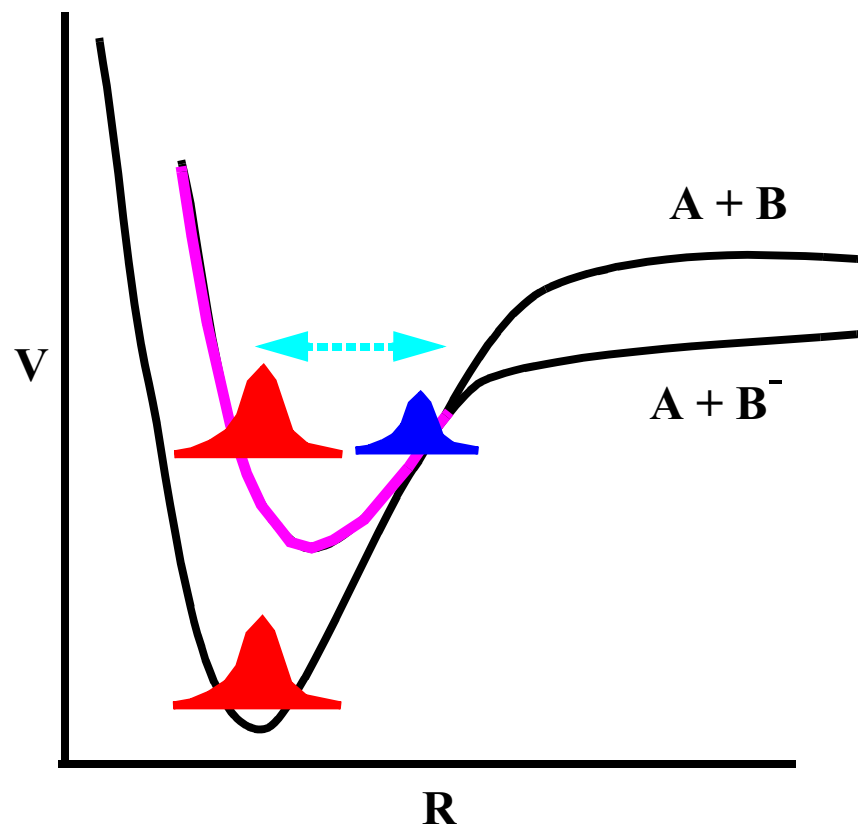
 **Local complex potential**

Scattering amplitude and cross section:

$$T_{f,i}(E) = \langle \Phi_{final} | \frac{1}{E - H_{anion}} | \Phi_{initial} \rangle$$

$$\sigma_{f,i}(E) = \frac{4\pi^3}{k^2} |T_{f,i}(E)|^2$$

Local Complex Potential or “Boomerang” model for Resonant Vibrational Excitation in 1D (diatomics)



Time-dependent formulation $\Phi_{initial}(R) = \left(\frac{\Gamma(R)}{2\pi}\right)^{1/2} \chi_i(R)$

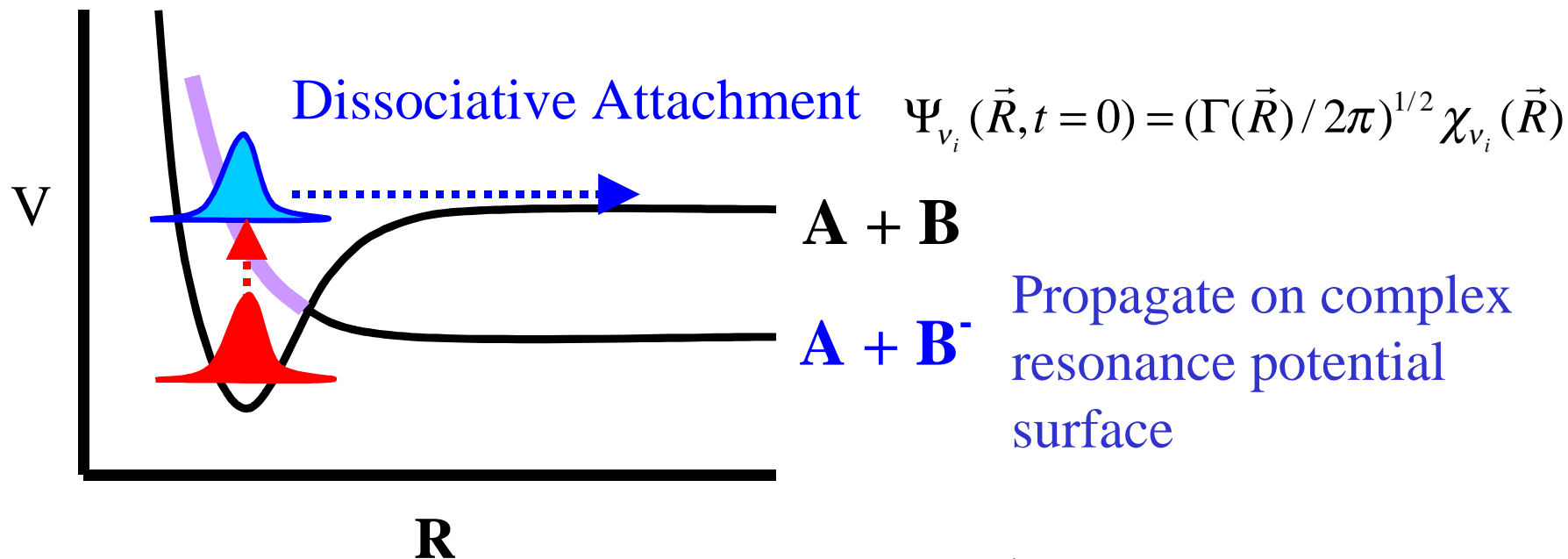
$$T_{f,i}(E) = -i \int_0^{\infty} e^{iEt} \langle \Phi_{final} | \Psi_t \rangle dt$$

with

$$\Psi_t = e^{-iH_{anion}t} |\Phi_{initial}\rangle$$

Local Complex Potential Model $W(\mathbf{R}) = E_{\mathbf{R}}(\mathbf{r}, \mathbf{R}, \gamma) - i \Gamma(\mathbf{r}, \mathbf{R}, \gamma)$

$$(E_{v_i} + k^2 / 2 - T - W(\vec{R}))\xi(\vec{R}) = (\Gamma(\vec{R}) / 2\pi)^{1/2} \chi_{v_i}(\vec{R})$$



Solution, $\zeta(\mathbf{R})$, is Fourier Transform

$$\xi(\vec{R}) = \lim_{\varepsilon \rightarrow \infty} i \int_0^\infty e^{i(E_{v_i} + k^2 / 2 + i\varepsilon)t} \Psi_{v_i}(\vec{R}, t) dt$$

Cross section from the asymptotic behavior of $\zeta(\mathbf{R})$

$$\sigma_{DA}^{jv}(k^2 / 2) = \frac{2\pi^2}{k^2} \frac{\kappa}{\mu_R} \lim_{R \rightarrow \infty} |P_{jv} \zeta(\vec{R}) R|^2$$

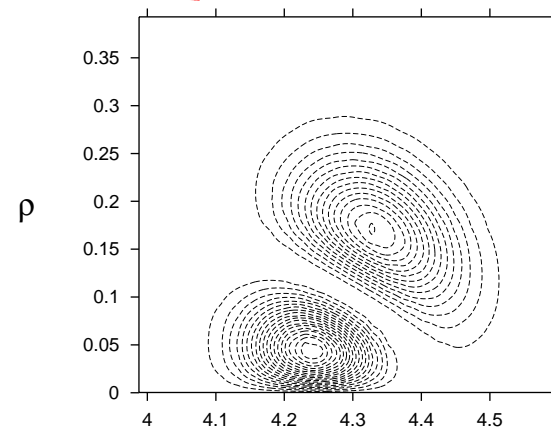
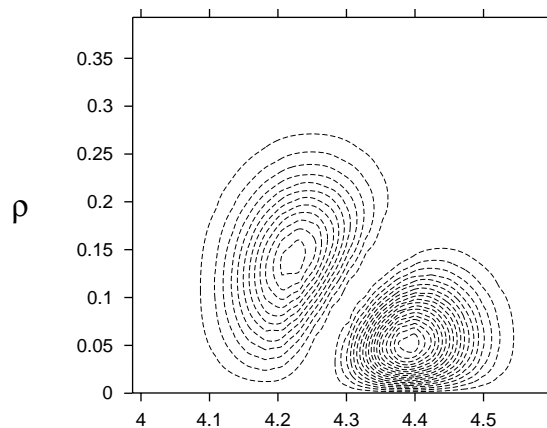
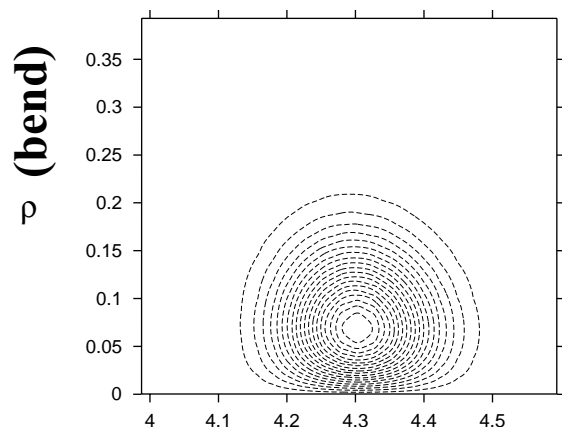
An Electron- CO₂ Primer

- CO₂ is linear in equilibrium geometry $R_{CO} = 2.1944 a_0$
- At the equilibrium geometry of CO₂, CO₂⁻ is an **unbound $2\Pi_u$ resonance state** (~3.8 eV above CO₂)
- The resonance state is doubly degenerate in linear geometry, but the degeneracy is lifted upon bending (Renner-Teller coupled states, **$2A_1$ and $2B_1$**)
- A low-energy enhancement in elastic scattering comes from a CO₂⁻ **virtual state** (confirmed by Morgan in 1998)
- CO₂⁻ is **bound** in linear geometry for CO bond distances greater than **$\sim 2.5 a_0$**
- CO₂⁻ is **bound** for R_{CO} = equilibrium value when it is bent by **~ 25 degrees**

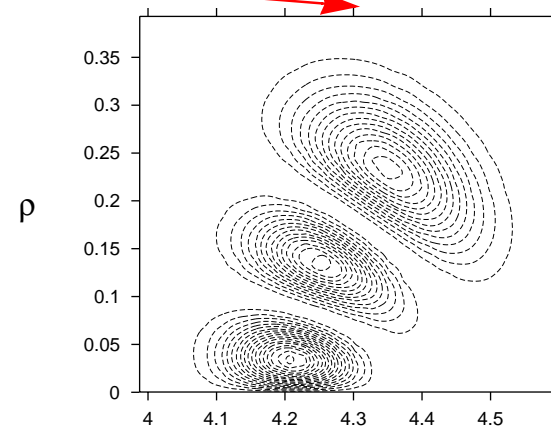
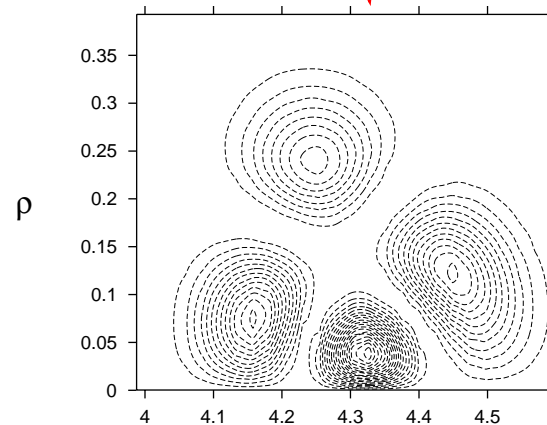
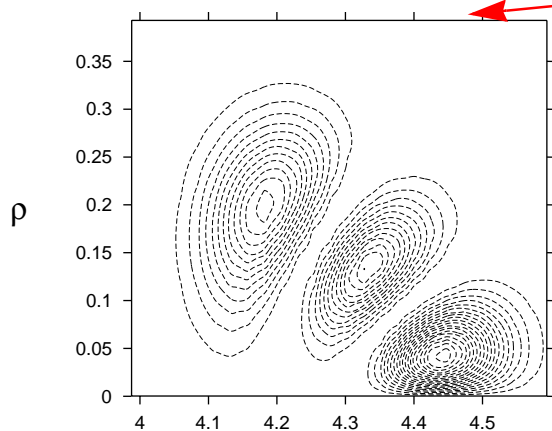
Vibrational states of CO₂ -- Near degeneracy of $\nu_{\text{stretch}} \sim 2\nu_{\text{bend}}$

(0,0,0)

Fermi dyad {coupled $(1,0^0,0)/(0,2^0,0)$ }



Fermi triad { $(2,0^0,0)/(1,2^0,0)/(0,4^0,0)$ }



Recent
Experi-
ments --
M.
Allan
2002

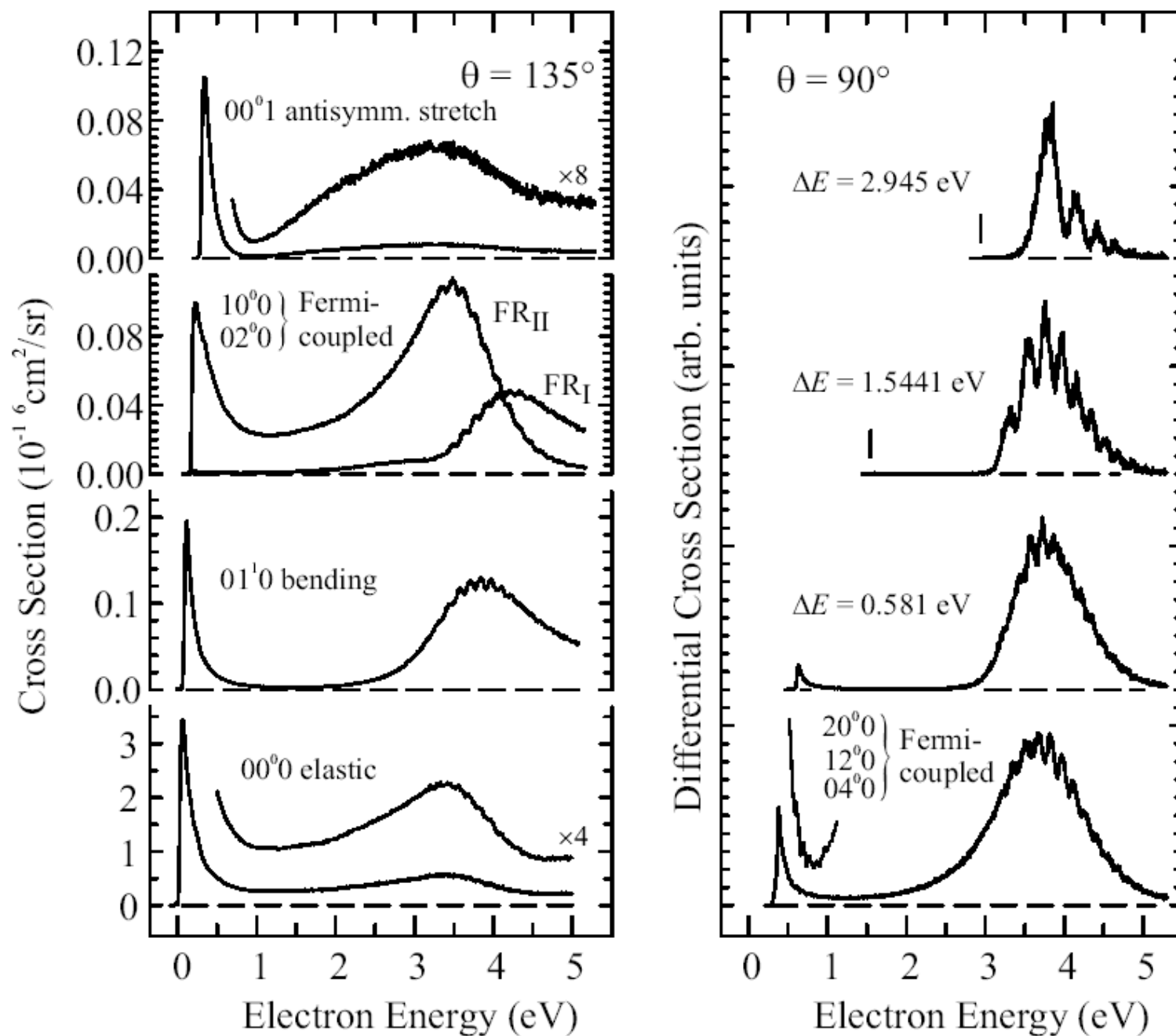
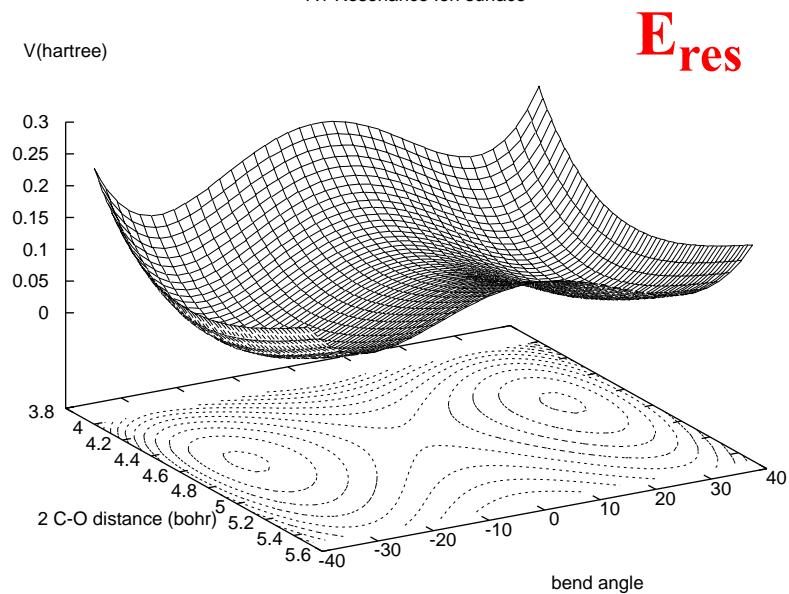


Figure 1. Overview of the elastic and vibrationally inelastic cross sections in CO₂. Reproduced from Allan (2002).

Complex Potential Surfaces for 2A_1 and 2B_1 resonance states

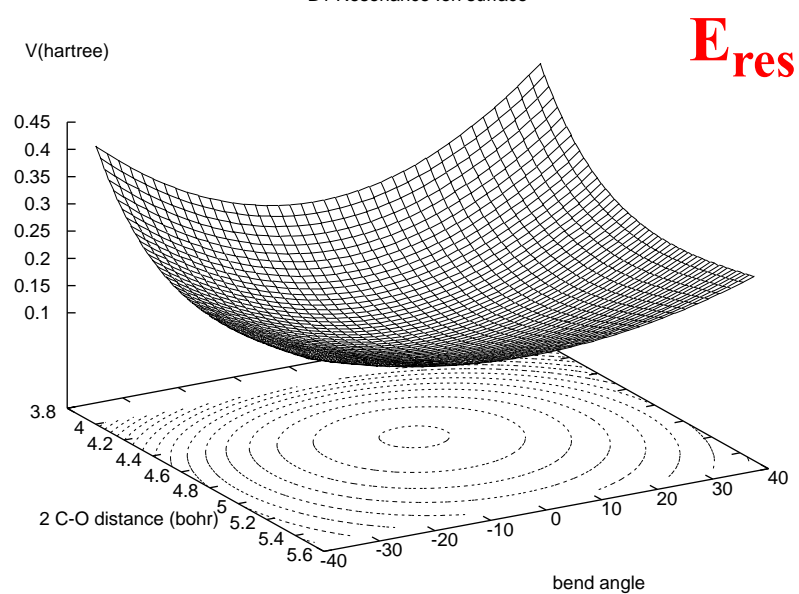
2A_1

A1 Resonance Ion surface

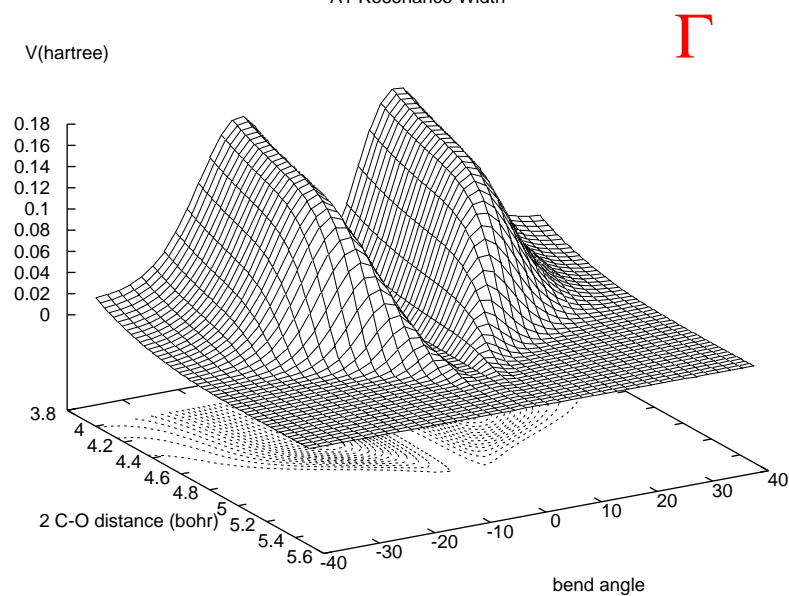


2B_1

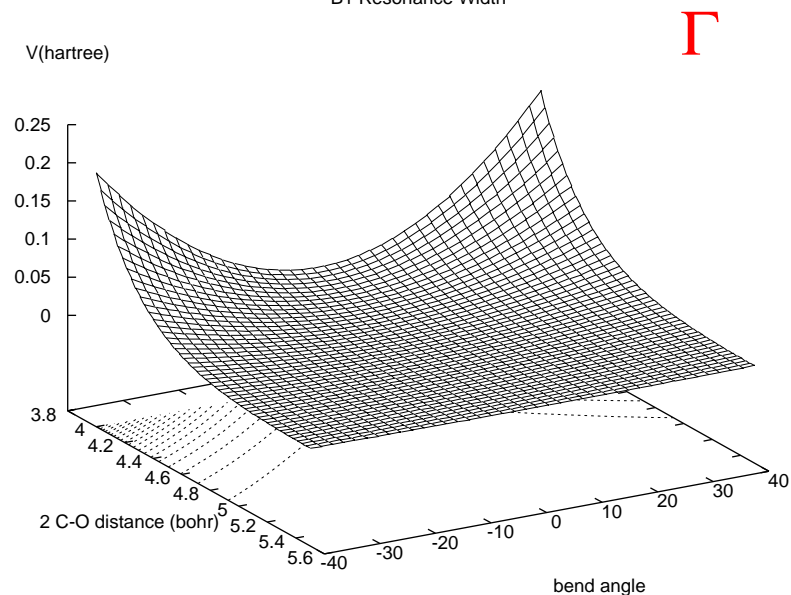
B1 Resonance Ion surface



A1 Resonance Width



B1 Resonance Width



Multiple Resonances and Renner-Teller Coupling

Upon bending the $^2\Pi_u$ state splits into two resonances, 2A_1 and 2B_1 .

- The Born Oppenheimer approximation breaks down and these two states are coupled by an effect first characterized by Renner and Teller in 1934.

Normal Coordinates for CO₂

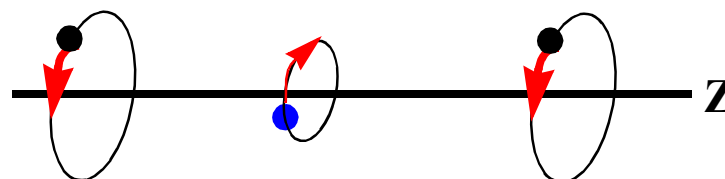
R = CO bond length

Θ = bend angle of CO from linear

$s = 2R \cos(\Theta)$ - Symmetric Stretch

$\rho = R^2 \sin^2(\Theta) / (1 + m_C / (2m_O))^2$ - bend

Degenerate Bending Modes



Degenerate bending modes can combine to give an angular momentum around the figure axis

Nuclear angular momentum K and electronic orbital angular momentum

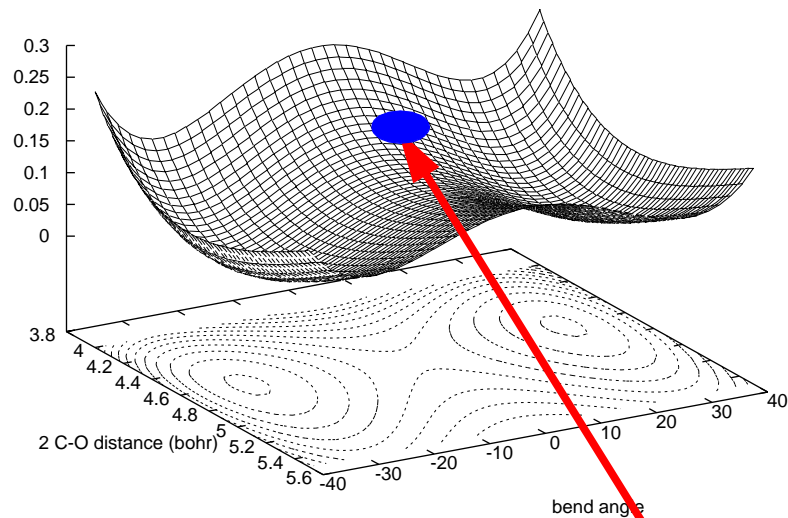
L give total angular momentum around the molecular axis $J_z = K_z + L_z$

resulting in “Renner-Teller” coupling proportional to $J_z L_z / \rho^2$

$2A_1$

A1 Resonance Ion surface

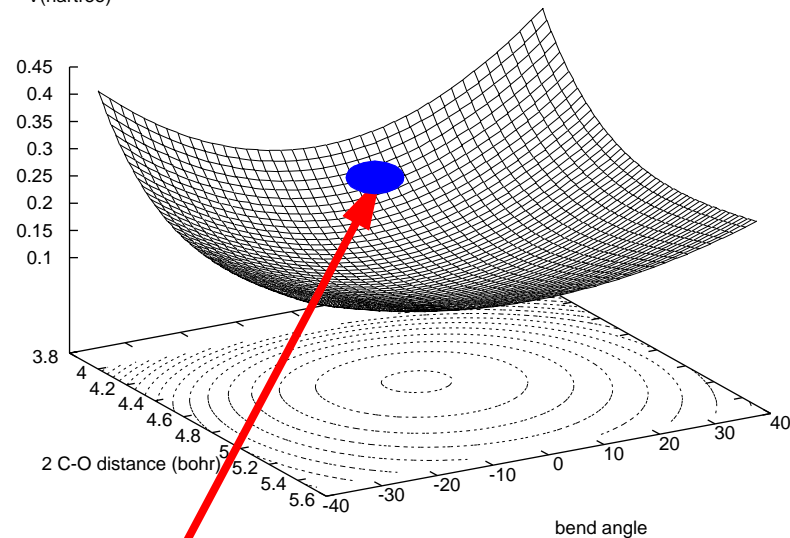
V(hartree)



$2B_1$

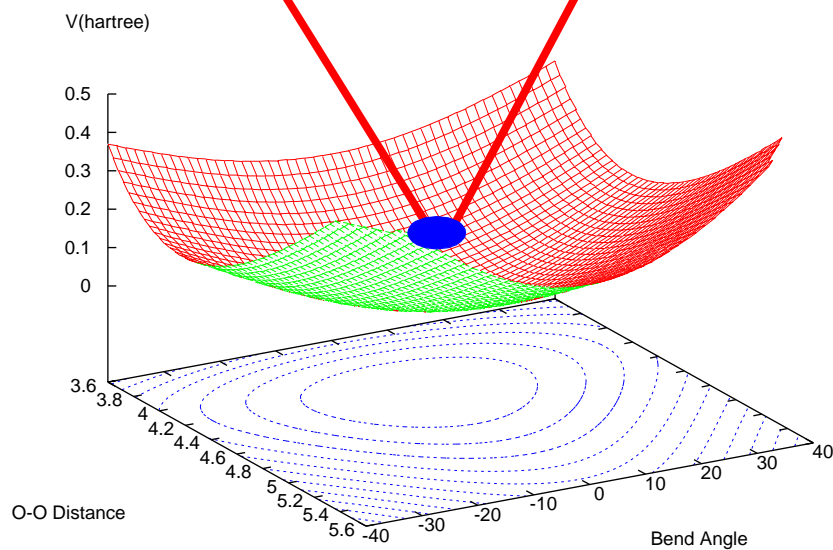
B1 Resonance Ion surface

V(hartree)



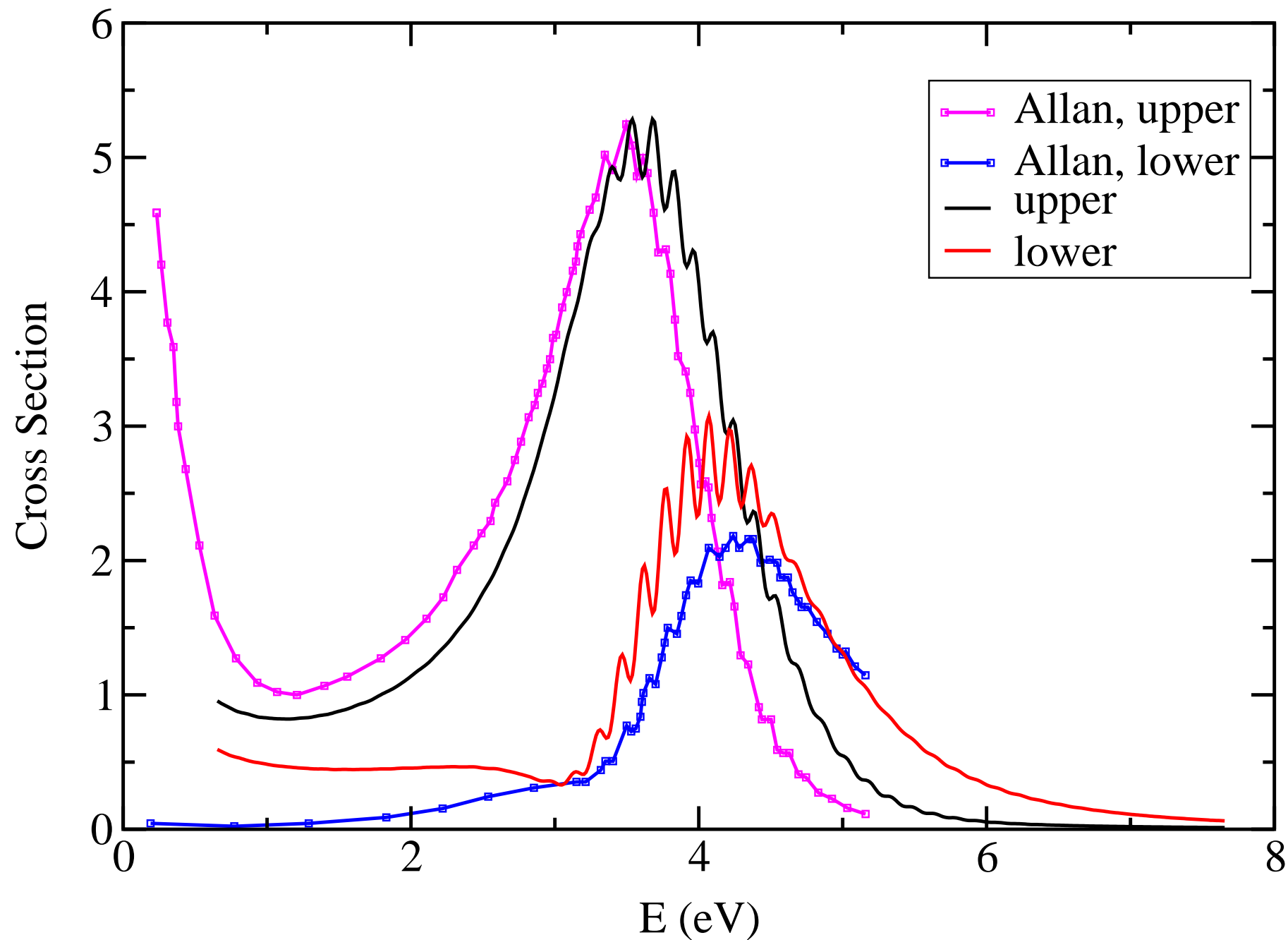
Multiple Resonance
“Boomerang”
approximation

Ground State Surface



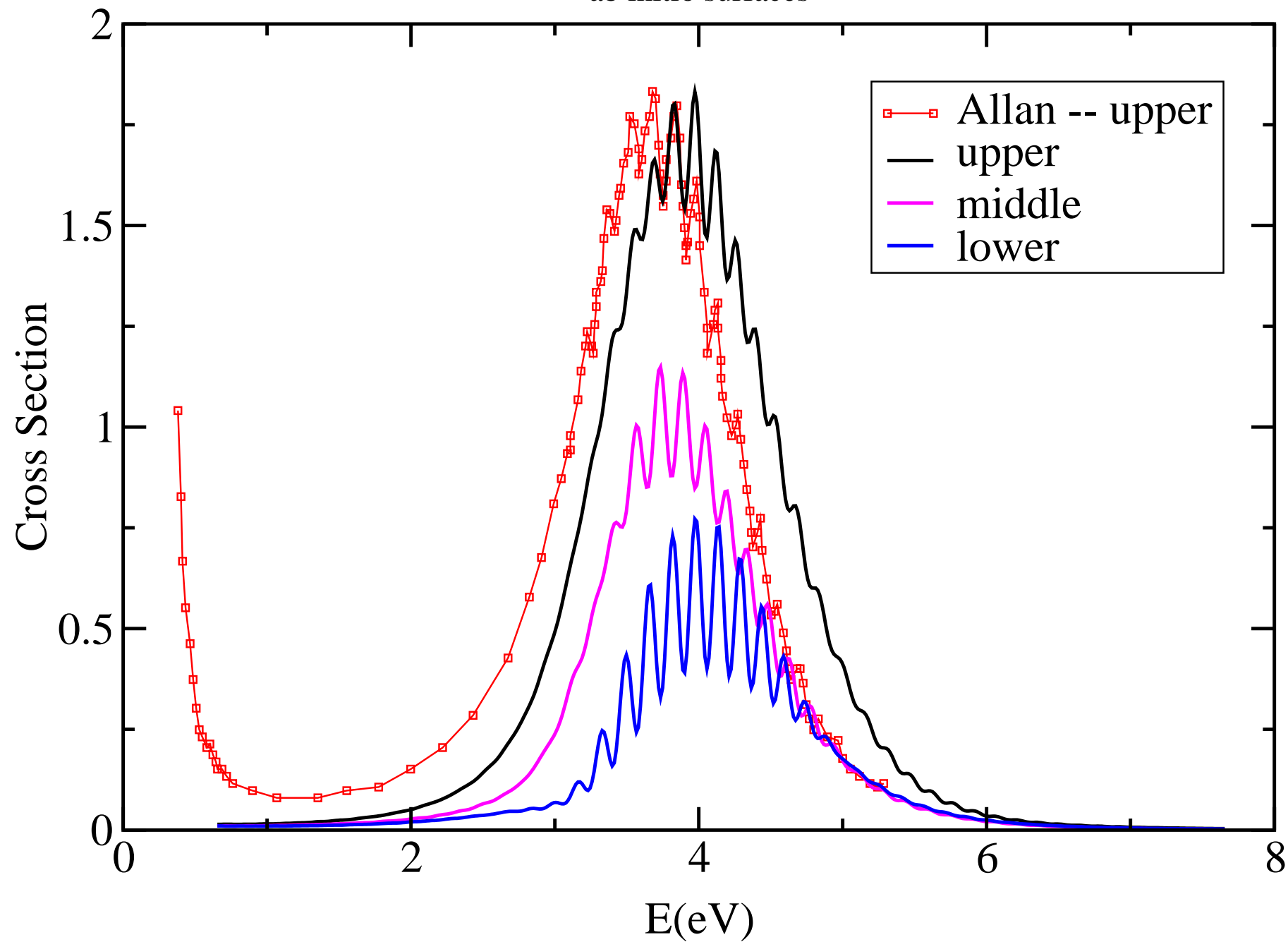
Excitation of First Fermi Dyad

Fully ab initio surfaces



Excitation of lowest Fermi Triad

ab initio surfaces



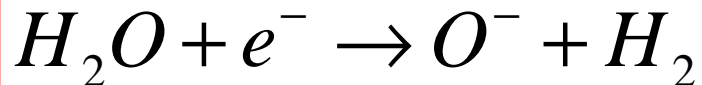
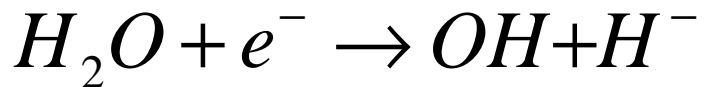
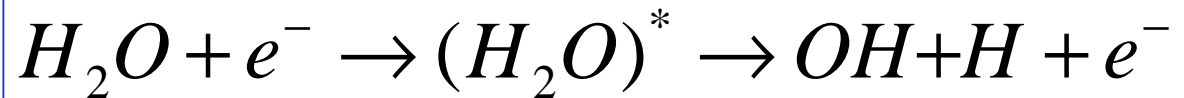
Some of what we have learned about electron-CO₂ collisions

- The resonance structure is an intrinsically polyatomic effect -- 1D models cannot account for it. The physical vibrational states of CO₂ are Fermi polyads that mix the bending and symmetric stretching modes.
- Motion on the A₁ surface alone cannot account for the resonance interference (“Boomerang”) structure in the cross sections.
- Renner-Teller coupling of ²A₁ and ²B₁ resonance states is necessary to describe the nuclear dynamics during resonant collisions.

A primer on the electron-driven chemistry of water

- The ground state configuration of water is
 - $1a_1^2 2a_1^2 1b_2^2 3a_1^2 1b_1^2$ 1A_1
- Electron-driven chemistry through both dissociative excitation and dissociative attachment

Electron impact
dissociation



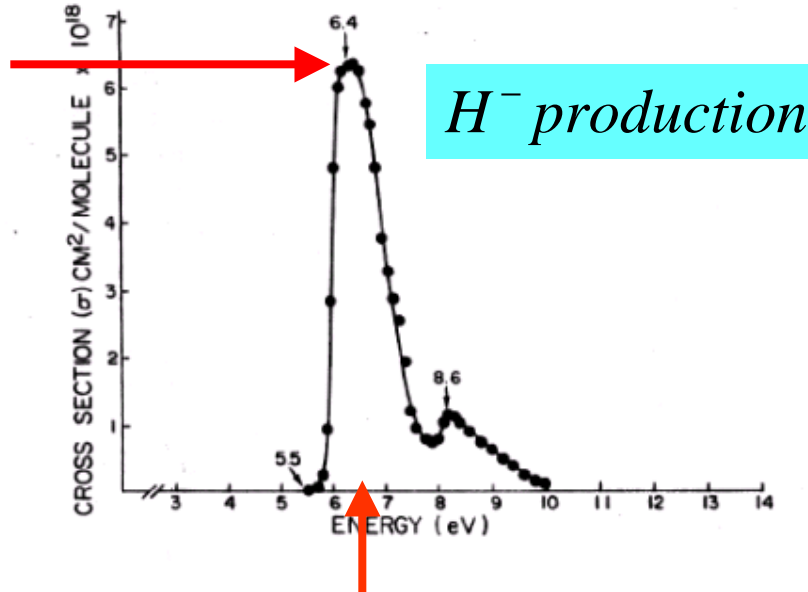
Dissociative
Attachment

Simple molecular orbital picture of the dissociation processes

- Dissociative excitation proceeds by excitation of low-lying dissociative electronic states, e.g, those observed in EELS spectra:
 - $1a_1^2 2a_1^2 1b_2^2 3a_1^2 \mathbf{1b_1^1} \mathbf{4a_1^1}$ $^{1,3} B_1$
 - $1a_1^2 2a_1^2 1b_2^2 \mathbf{3a_1^1} \mathbf{1b_1^2} \mathbf{4a_1^1}$ $^{1,3} A_1$
- Dissociative attachment of H_2O proceeds through Feshbach resonances
 - $1a_1^2 2a_1^2 1b_2^2 3a_1^2 \mathbf{1b_1^1} \mathbf{4a_1^2}$ 2B_1 (~ 6.5 eV)
 - $1a_1^2 2a_1^2 1b_2^2 \mathbf{3a_1^1} \mathbf{1b_1^2} \mathbf{4a_1^2}$ 2A_1 (~ 9 eV)
 - $1a_1^2 2a_1^2 \mathbf{1b_2^1} \mathbf{3a_1^2} \mathbf{1b_1^2} \mathbf{4a_1^2}$ 2B_2 (~ 12 eV)

H^- production is primarily through the 2B_1 Resonance

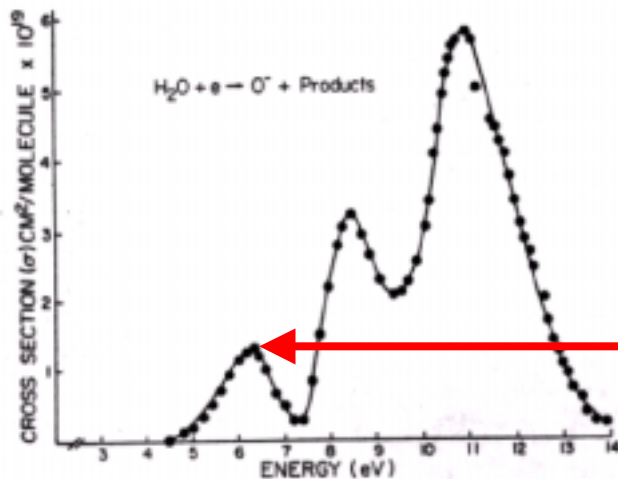
$$\approx 6.5 \times 10^{-18} \text{ cm}^2$$



H^- production

C. E. Melton, Journal of Chemical Physics, **57**, pp.4218-25, (1972).

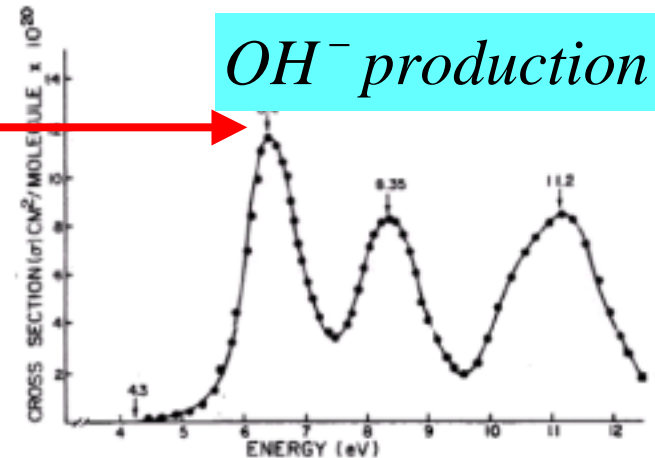
O^- production



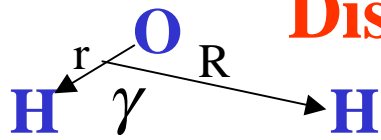
$$\approx 1.2 \times 10^{-19} \text{ cm}^2$$

$$\approx 1.5 \times 10^{-19} \text{ cm}^2$$

OH^- production



A Complete *ab initio* Treatment of Polyatomic Dissociative Attachment: 2B_1 Resonance



1. Electron scattering: Calculate the energy and width of the resonance for fixed nuclei
 - Complex Kohn calculation of fixed-nuclei electron scattering cross sections – produce $\Gamma(r, R, \gamma)$
 - CI calculations -- produce $E_{\text{Re}}(r, R, \gamma)$
2. Fitting of complete resonance potential surface including the electronically bound (product) regions
3. Nuclear dynamics in the local complex potential model on the anion surface $V_{\text{anion}} = E_R(r, R, \gamma) - i\Gamma(r, R, \gamma)/2$
 - Multiconfiguration Time-Dependent Hartree (MCTDH)
 - Flux correlation function calculation of DA cross sections

Configuration Interaction calculation for real part of the 2B_1 (${}^2A''$) resonance surface

- Real part of resonance energy, $E_R(r,R,\gamma)$, nearly parallels the “parent” 3B_1 state
- When the resonance becomes bound, the CI calculation of $E_R(r,R,\gamma)$ must dissociate properly
- Dominant configuration is $1a_1^2 2a_1^2 1b_2^2 3a_1^2$ **$1b_1^1 4a_1^2$**
- A robust basis set is necessary: **au-cc-pvTZ**

CI (898,075 configurations):

- Singles and doubles excitation from the CAS reference space

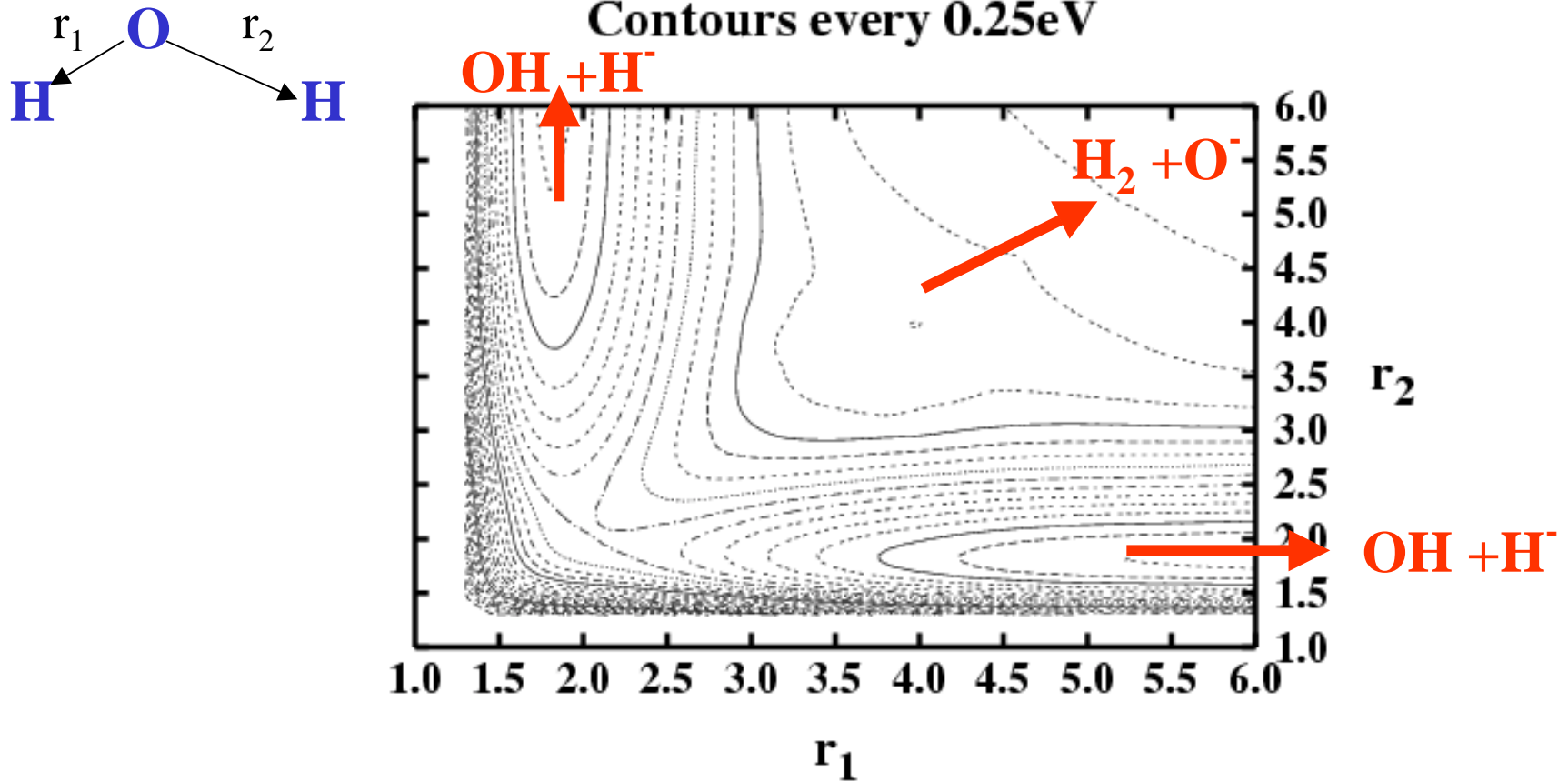
$(1b_2, 3a_1, 1b_1, 4a_1, 5a_1, 2b_2)^7$

- **$4a_1$** is the “resonance” orbital,
- **$5a_1$** is an important correlation orbital,
- **$2b_2$** for the correct dissociation

Entire 2B_1 ($^2A''$) potential surface is fit with combination analytic fit and 3-D spline.

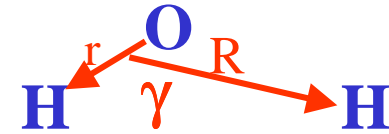
PES in valence-bond coordinates at $\theta=1.83$

Contours every 0.25eV



$$V^{Fit}(r_1, r_2, \vartheta) = V_{Morse}(r_1) + V_{Morse}(r_2) + V_{Morse}(r_{H-H}) + f_{3DSpline}(r_1, r_2, \vartheta)$$

Hamiltonian for Nuclear Motion



- For $J = 0$ the wave function is a function of only internal coordinates $\Psi^{J=0}(r, R, \gamma)$

$$H^{J=0} = -\frac{1}{2\mu_R} \frac{\partial^2}{\partial R^2} - \frac{1}{2\mu_r} \frac{\partial^2}{\partial r^2} + \frac{\hat{j}^2}{2\mu_r r^2} + \frac{\hat{j}^2}{2\mu_R R^2} + W(r, R, \gamma)$$

- For arbitrary J : $\Psi^{JM}(r, R, \gamma, \alpha, \beta, \zeta) = \sum_K \psi^{JK}(r, R, \gamma) D_{KM}^J(\alpha, \beta, \zeta)$

$$H_{KK}^J = -\frac{1}{2\mu_R} \frac{\partial^2}{\partial R^2} - \frac{1}{2\mu_r} \frac{\partial^2}{\partial r^2} + \frac{\hat{j}^2}{2\mu_r r^2} + \frac{1}{2\mu_R R^2} [J(J+1) - 2K^2 + \hat{j}^2] + V(r, R, \gamma)$$

$$H_{K\pm 1, K}^J = \frac{1}{2\mu_R R^2} \sqrt{J(J+1) - K(K\pm 1)} \hat{j}_{\pm}$$

Solving the multidimensional Time-Dependent Schrödinger Equation

- Multi-configuration time-dependent Hartree (MCTDH) method in collaboration with Prof. H. Dieter-Meyer, University of Heidelberg
- **Start with a time-independent orthonormal product basis**

$$\{\chi_{j_1}^{(1)}(Q_1) \dots \chi_{j_f}^{(f)}(Q_f)\} \quad j_i = 1 \dots N_i$$

- **The MCTDH wave function is a time-dependent linear combination of configurations**

$$\Psi(Q_1, \dots, Q_f, t) = \sum_{j_1=1}^{n_1} \dots \sum_{j_f=1}^{n_f} A_{j_1 \dots j_f}(t) \prod_{\kappa=1}^f \varphi_{j_\kappa}^{(\kappa)}(Q_\kappa, t) \quad n_\kappa \ll N_\kappa$$

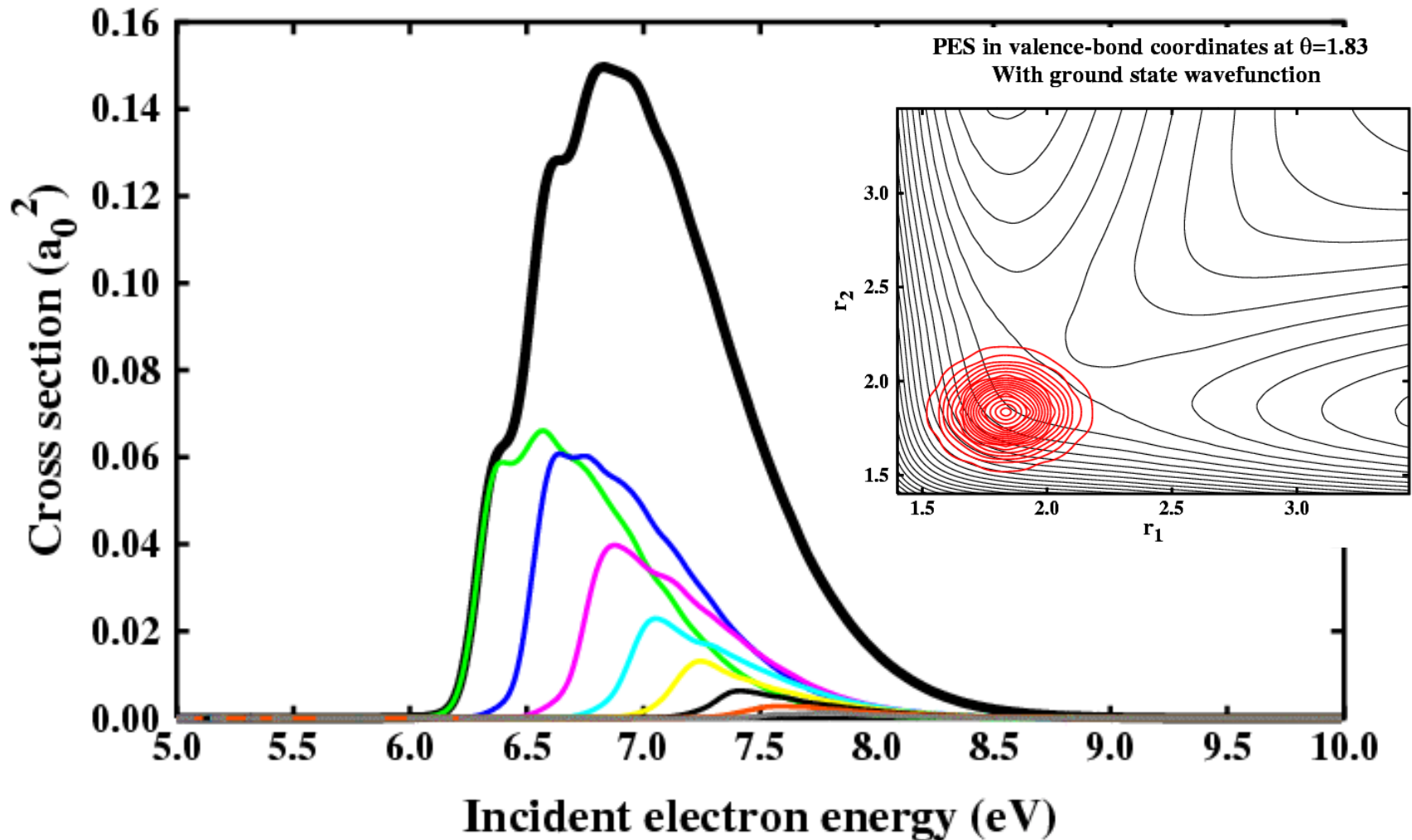
- **The time-dependent single-particle functions are represented as**

$$\varphi_{j_\kappa}^{(\kappa)}(Q_\kappa, t) = \sum_{i_\kappa=1}^{N_\kappa} c_{i_\kappa j_\kappa}^{(\kappa)}(t) \chi_{i_\kappa}^{(\kappa)}(Q_\kappa)$$

- **Derive equations of motion for both the coefficients $A_{j_1 \dots j_f}(t)$ and the single-particle functions $\varphi_{j_\kappa}^{(\kappa)}(Q_\kappa, t)$**

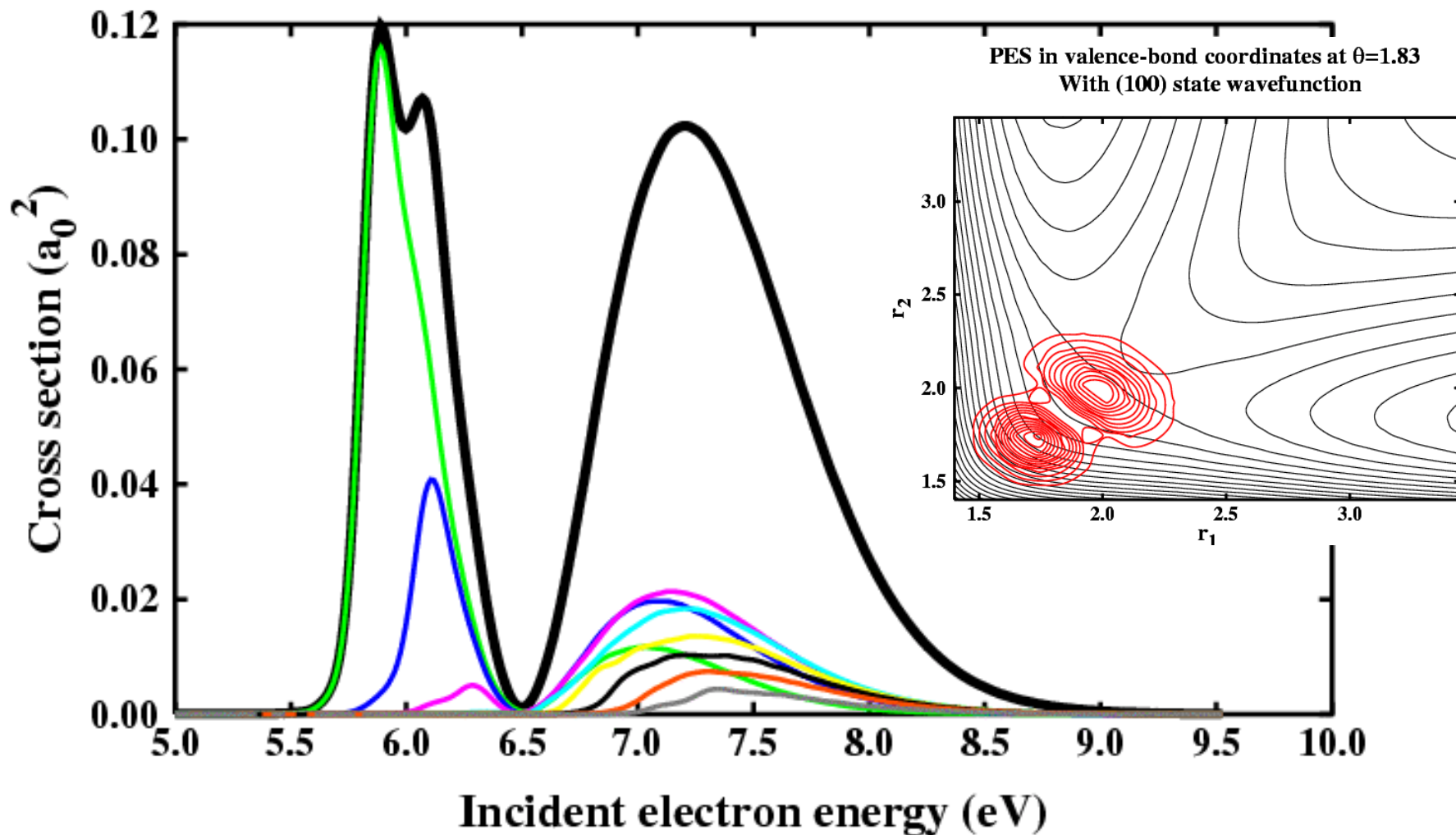
H⁻ production from the ground state of H₂O

DA cross section for H⁻ + OH from ground state
Total and into each OH vibrational state

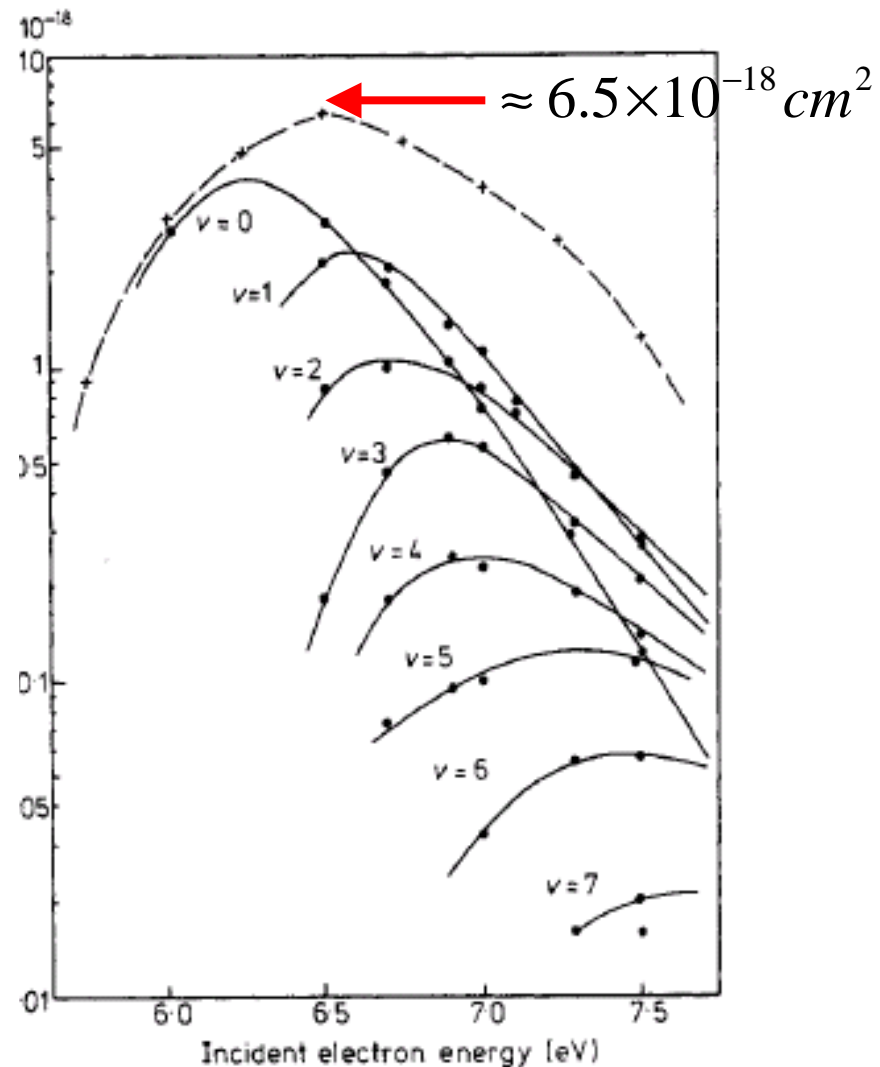
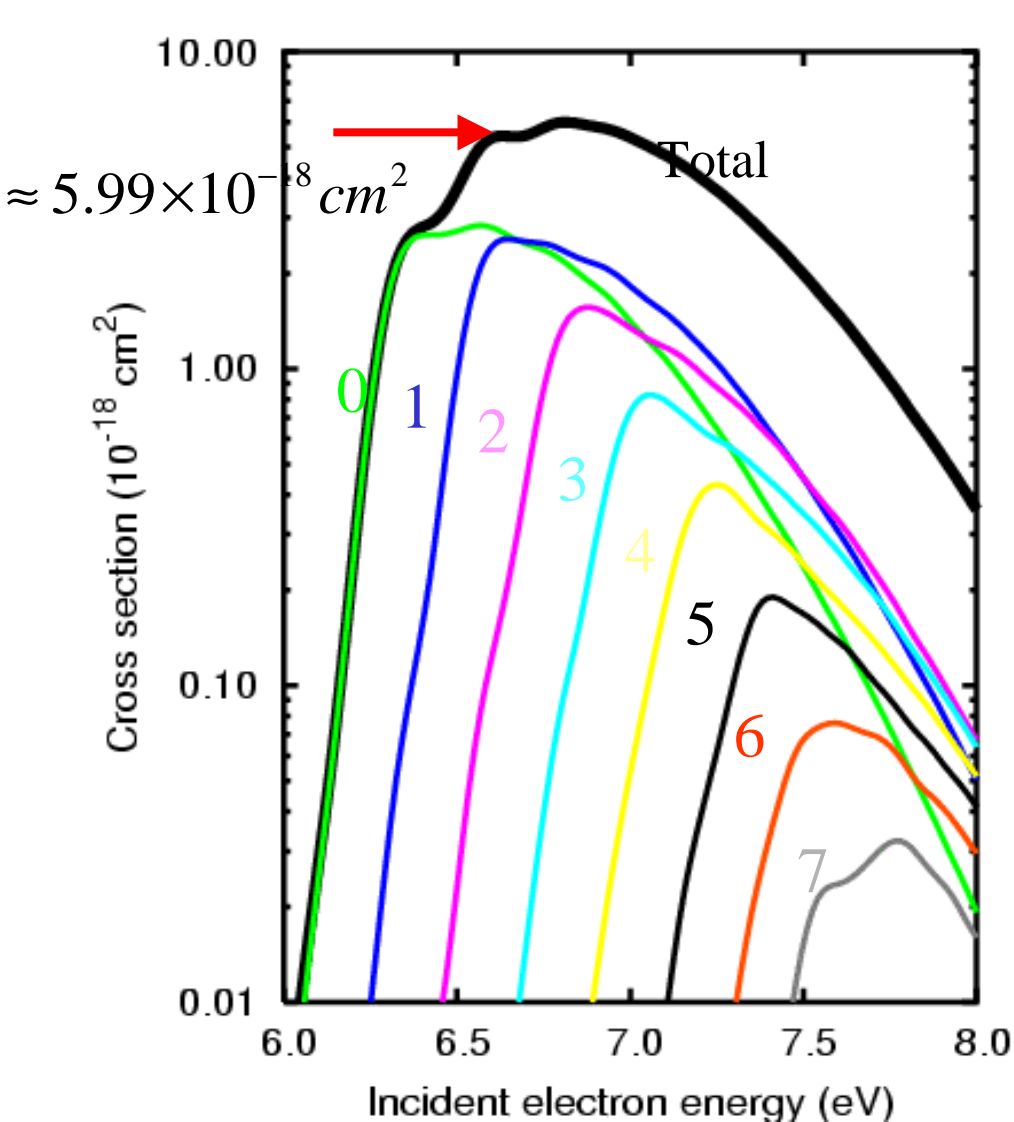


H⁻ from single excitation of symmetric stretch

DA cross section for H⁻ + OH from (100) state
Total and into each OH vibrational state

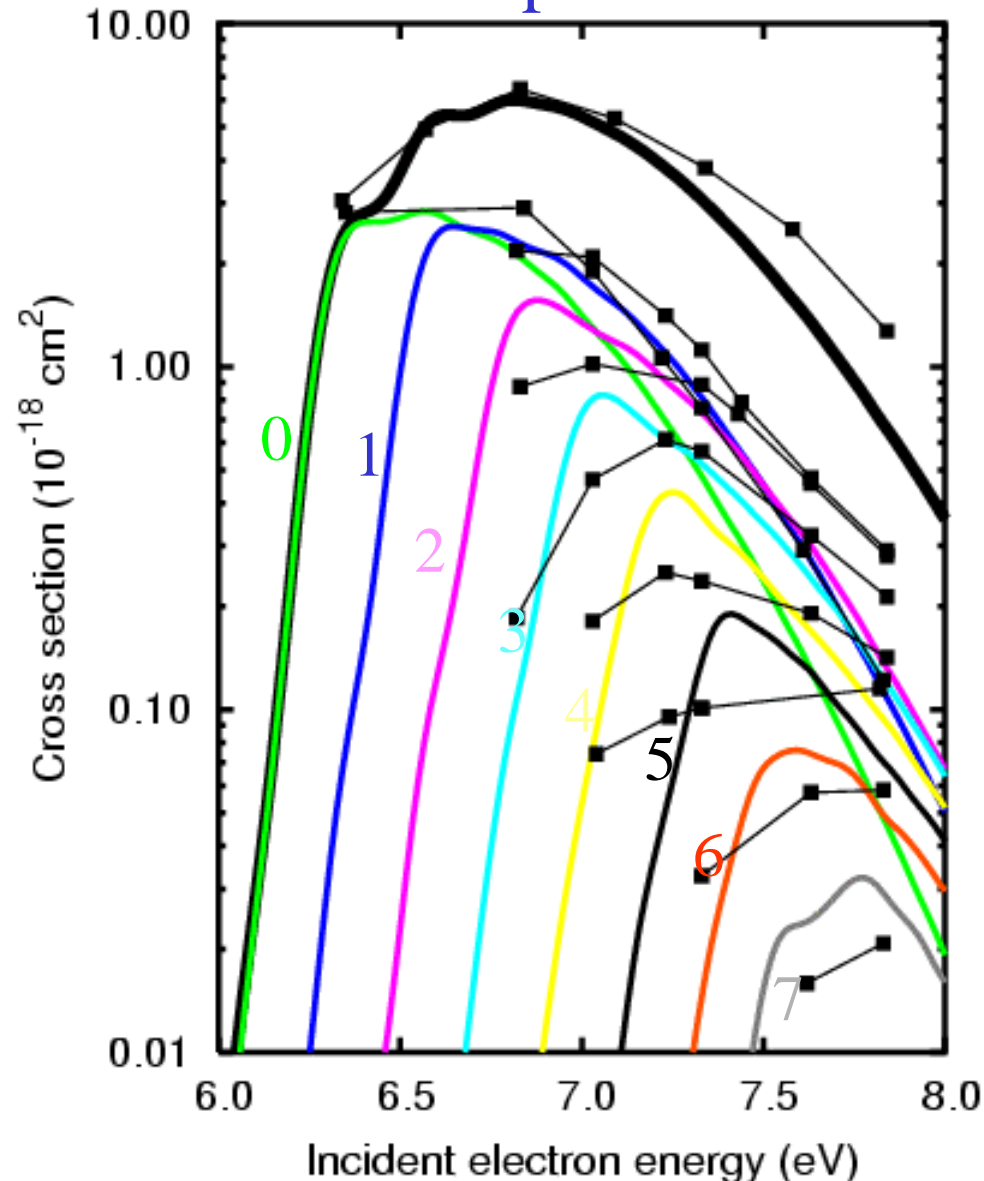


Cross Sections for OH vibrational states compared with experiment



D. S. Belic, M. Landau and R. I. Hall, Journal of Physics B **14**, pp.175-90 (1981)

Cross Sections compared with experiment – experiment shifted +0.34eV to match peak of total cross section



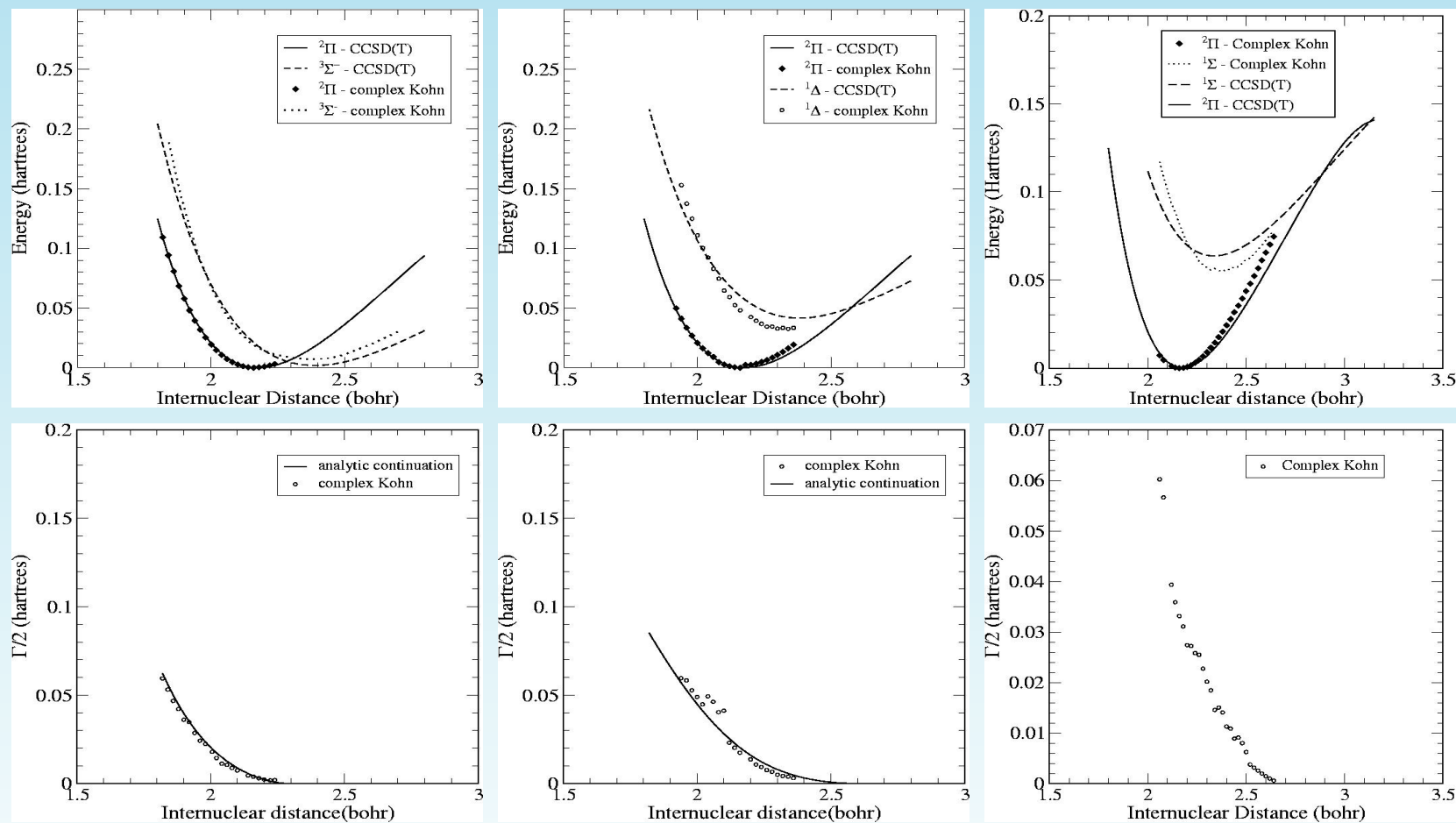
Conclusions and Open Questions

- It is now possible to treat dissociative attachment to a triatomic in full dimensionality from first principles.
- Dynamics of the 2B_1 ($^2A''$) resonance leads almost exclusively to $H^- + OH$
- An ab initio treatment reproduces the cross sections for producing OH in excited vibrational states to within a factor of 2
- Interesting energy dependence is predicted for cross sections from H_2O excited in symmetric stretch
- The dynamics of the other two resonances (2A_1 and 2B_2) remains unknown.
- Is there production of O^- from Renner-Teller or other nonadiabatic coupling between resonances? Are other nonadiabatic couplings important?
- Rotational excitation of OH still difficult to compute in these calculations (long-range charge dipole interaction).

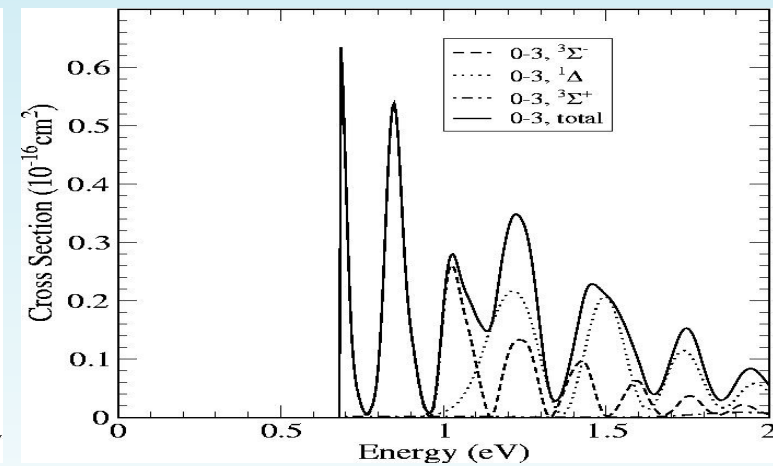
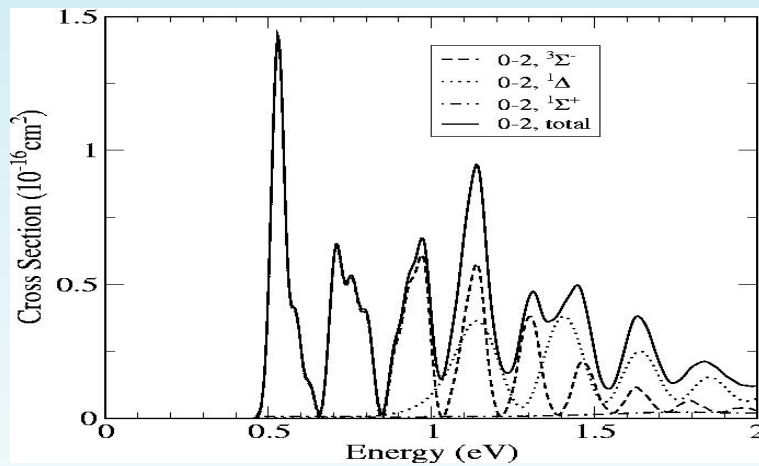
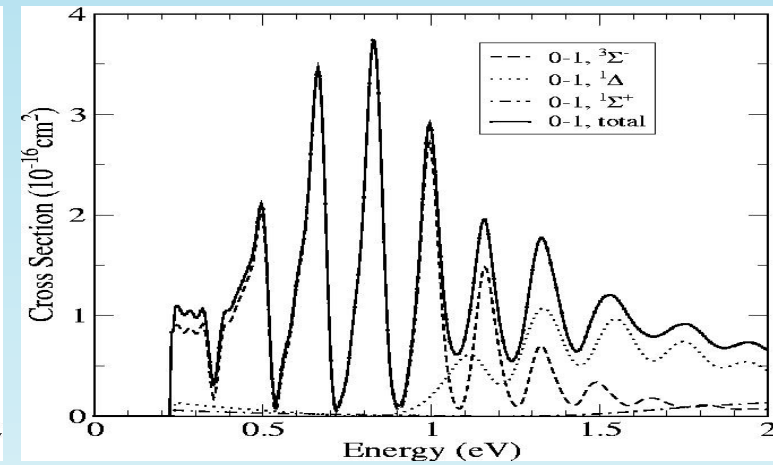
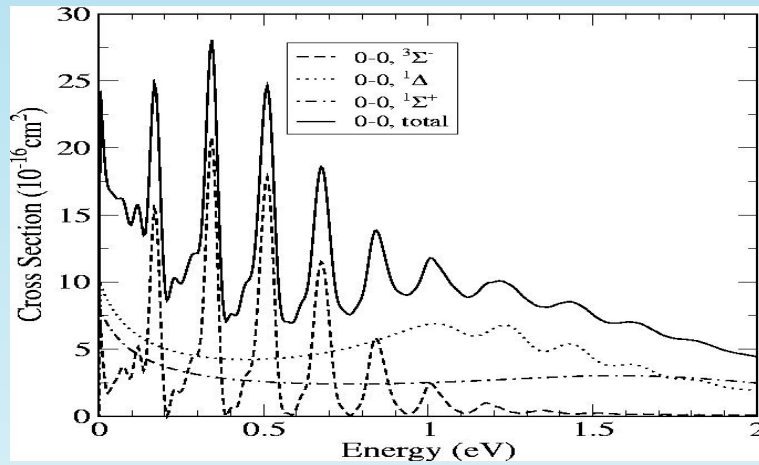
The e^- -NO Example: Overlapping Low-Energy Resonances

- e^- -NO scattering below 2 eV is dominated by shape resonances
- NO has an open-shell (2π) ground-state
- By analogy with O_2 , one expects three low-lying ($2\pi^2$) negative ion states - $^3\Sigma^-$, $^1\Delta$ and $^1\Sigma^+$
- e^- -NO presents significant challenges to contemporary scattering theory
 - ★ Careful balance of correlation effects in N and (N+1)-electron systems requires elaborate wave functions
 - ★ Quantitative treatment of scattering at low energies requires non-local treatment beyond the Boomerang model

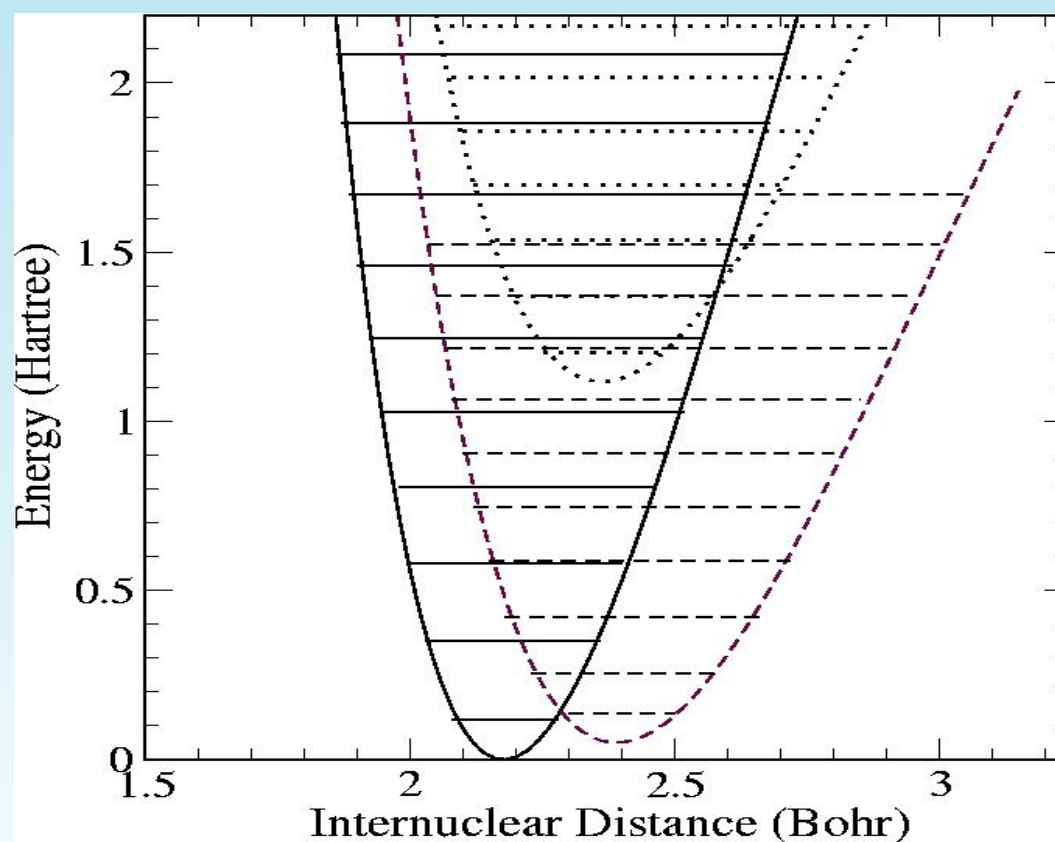
NO/NO⁻ Potential Curves and Widths



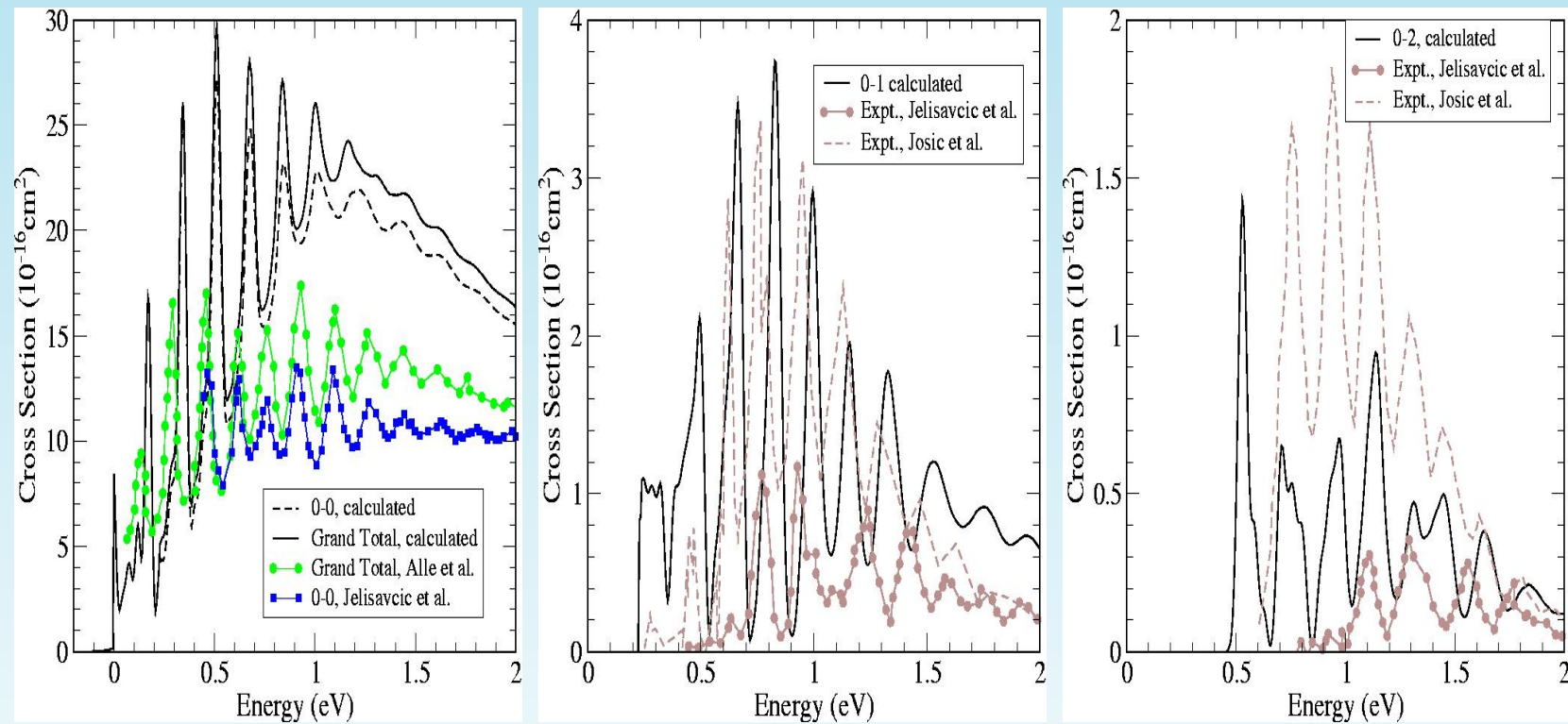
Electron-NO Vibrational Cross Sections



NO Neutral and Anion Potential Curves and Vibrational Levels



Electron-NO Cross Sections: Theory and Experiment



Conclusions

- *ab initio* results confirm that the prominent features in the elastic and vibrational excitation cross sections arise from $^3\Sigma^-$ and $^1\Delta$ negative ion states.
- The lowest energy peaks observed are due to the $^3\Sigma^-$ state and appear at the same energy in different exit channels.
- The $^3\Sigma^-$ peaks are overlapped by a broader series of $^1\Delta$ peaks at higher energies which shift in energy as the exit channel quantum number changes.
- The third $^1\Sigma^+$ resonance, which contributes to the elastic background cross section, is too broad to display any boomerang structure.

Beyond the Local Boomerang Model

- The vibrational levels of the $^3\Sigma^-$ anion are energetically close to those of the neutral target, which invalidates several key assumptions used in deriving the local complex potential model.
- Non-local effects, beyond the boomerang model, may be critical in explaining the suppression of resonance peaks that occurs in the higher excitation cross sections.